REPORT 1000

CALCULATION OF THE AERODYNAMIC LOADING OF SWEPT AND UNSWEPT FLEXIBLE WINGS OF ARBITRARY STIFFNESS [1]

By Franklin W. Diederich

SUMMARY

A method is presented for calculating the aerodynamic loading, the divergence speed, and certain stability derivatives of swept and unswept wings and tail surfaces of arbitrary stiffness. Provision is made for using either stiffness curves and root-rotation constants or structural influence coefficients in the analysis. Computing forms, tables of numerical constants required in the analysis, and an illustrative example are included to facilitate calculations by means of the method.

INTRODUCTION

The distribution of the aerodynamic loading on wings and tail surfaces is important both for the structural analysis of these components, since it determines the applied bending moment and torque acting at any station, and for their aerodynamic analysis, since it affects the stability derivatives to a large extent. At high speeds the aerodynamic loading, particularly in the case of swept wings, is greatly affected by the structural deformations caused by the loading. The present report is concerned with the determination of the effects of structural flexibility on the aerodynamic loading of wings of arbitrary plan form and stiffness.

The present report treats the problem of aerodynamic loading by matrix methods. Aerodynamic induction is taken into account by means of approximate aerodynamic influence coefficients. When more accurate coefficients become available, they can readily be incorporated in this method. Structural flexibility is taken into account in the form of either calculated stiffness variations or measured influence coefficients. The required integrating matrices are presented for both a six-point and a ten-point solution. For the six-point solution convenient computing forms are included as well. The method is illustrated by means of an example. In addition to the analysis of the aerodynamic loading, the determination of the related divergence speed and of certain stability derivatives is discussed.

For the convenience of the reader unfamiliar with matrix terminology, a summary of matrix methods has been included in the appendix. The sections entitled "Application of the Method" and, in particular, "Instructions for Solution" may be read without reference to the section entitled "Derivation of the Method."

SYMBOLS

A	aspect ratio $\left(\frac{b^2}{S}\right)$
$[A], [A^1]$	aeroelastic matrices defined by equations (21) and (35)
a	section aerodynamic center, measured from leading edge, fraction of chord
b	wing span, inches
b'	wing span less fuselage width, inches
c	chord measured parallel to the air stream, inches
$\bar{c}$	average wing chord, inches $\left(\frac{S}{b}\right)$
c_l	section lift coefficient $\left(\frac{l}{qc}\right)$
c_{l_α}	section lift-curve slope, per radian
C_L	lift coefficient $\left(\frac{L}{qS}\right)$
C_{L_α}	wing lift-curve slope, per radian
$C_{L_{\alpha_e}}$	effective lift-curve slope for twist distributions, per radian
C_{BM}	root bending-moment coefficient $\left(4\frac{M_r}{qSb}\right)$
C_l	rolling-moment coefficient $\left(\frac{\text{Rolling moment}}{qSb}\right)$
$[C_1]$	matrix relating concentrated and accumulated torques
$[C_2]$	matrix relating concentrated loads and accumulated bending moments
$[C_3]$	matrix converting torques due to distributed loads to torques due to concentrated torques
$[C_4]$	matrix converting bending moments due to distributed loads to bending moments due to concentrated loads
EI	bending stiffness in planes perpendicular to the elastic axis, pound-inches^2
e	location of elastic axis measured from leading edge, fraction of chord
e_1	dimensionless distance along chord from reference axis to section aerodynamic center $(e-a)$
GJ	torsional stiffness in planes perpendicular to the elastic axis, pound-inches^2
$[I], [I']$	integrating matrices for single integration from tip to root
$[I_1]$	first row of matrix $[I]$

[1] Supersedes NACA TN 1876—Calculation of the Aerodynamic Loading of Flexible Wings of Arbitrary Plan Form and Stiffness, by Franklin W. Diederich, April 1949.

$[II]$,$[II']$ integrating matrices for double integration from tip to root

$[II_1]$ first row of matrix $[II]$

$[I]''$ integrating matrix for single integration from root to tip (double transpose of matrix $[I]$)

k dimensionless parameter $\left(\frac{(GJ)_r}{(EI)_r}\frac{b'/2}{e_{1_r}c_r\cos^2\Lambda}\tan\Lambda\right)$

κ wing lift-curve-slope ratio $(C_{L_{\alpha_s}}/C_{L_\alpha})$

L lift, pounds

l running air load per unit length perpendicular to the plane of symmetry, pounds per inch

M accumulated bending moment (about axes parallel to the plane of symmetry unless specified otherwise), inch-pounds

M_0 free-stream Mach number

P concentrated load, pounds

$\frac{pb}{2V}$ wing-tip helix angle

$[Q]$ aerodynamic influence-coefficient matrix

Q_α, Q_φ root-twist constants (see equation (15))

Q_Γ root-bending constant (see equation (15))

q dynamic pressure, pounds per square inch

q^* dimensionless dynamic pressure $\left(\frac{C_{L_\alpha}q(b'/2)^2e_{1_r}c_r^2\cos\Lambda}{(GJ)_r}\right)$

$q^\dagger$ reduced dynamic pressure $\left(C_{L_\alpha}q\frac{b'}{2}c_r\right)$

$\bar{q}$ dimensionless dynamic pressure $\left(\frac{C_{L_\alpha}q(b'/2)^3c_r\tan\Lambda}{(EI)_r\cos\Lambda}\right)$

S total wing area including part of wing covered by fuselage, square inches

s distance from wing root along reference axis, inches

T accumulated torque (about axes perpendicular to the plane of symmetry unless specified otherwise), inch-pounds

T_c concentrated torque, inch-pounds

t running torque due to air load about axes perpendicular to the plane of symmetry, inch-pounds per inch

w fuselage width, inches

w_e distance between the effective root and the innermost complete section of the torsion box perpendicular to the elastic axis, inches

y lateral ordinate measured from plane of symmetry, inches

$\bar{y}$ lateral center of pressure, inches

α angle of attack, radians

$\bar{\alpha}$ equivalent angle of attack, radians $\left(\alpha_s+\frac{C_{L_{\alpha_s}}}{C_{L_\alpha}}\alpha_s\right)$

Γ local dihedral angle due to deformation, or slope of wing deflection curve at reference axis, radians

ζ structural deflection, inches

η lateral distance from wing root, inches

Λ angle of sweepback (measured to the reference axis unless specified otherwise), degrees

$[\Phi_P]$ influence-coefficient matrix for wing twist in planes parallel to the air stream due to concentrated unit loads applied at the reference axis, radians per pound

$[\Phi_T]$ influence-coefficient matrix for wing twist in planes parallel to the air stream due to concentrated unit torques applied in planes parallel to the air stream, radians per inch-pound

φ angle of twist in planes perpendicular to the reference axis, radians

Subscripts:

$c/2$ midchord

D divergence

fw flexible wing

g geometric

LE leading edge

M due to bending moment

MAC pertaining to mean aerodynamic chord

P due to concentrated load

p damping in roll

r at root or effective root unless specified otherwise

rw rigid wing

s structural (due to structural deformations)

sub subsonic

spr supersonic

T due to torque

TE trailing edge

w wing exclusive of fuselage

Λ in or pertaining to sections perpendicular to the reference axis

Matrix notation:

$\{\ \}$ column matrix

$[\ ]$ row matrix

$[\ ]$ square matrix

$[\ ]$ diagonal matrix

$[\ ]'$ transpose of a matrix

$[\ ]''$ double transpose of a matrix: first about the principal diagonal, then about the other diagonal

$[1]$ unit matrix

$[1_1']$ matrix defined by equation (18)

DERIVATION OF THE METHOD

METHOD EMPLOYING STIFFNESS CURVES

Assumptions.—In the development of the method the following assumptions are made:

(a) All deflections and angles of attack are small.

(b) The wing is mounted flexibly at an effective root perpendicular to the elastic axis through the intersection of the elastic axis and the fuselage (see fig. 1), the root rotations being proportional to the root bending moment and root torque.

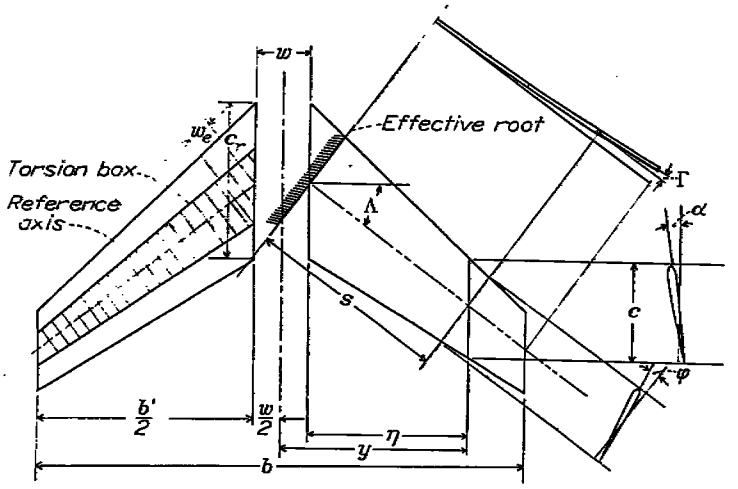

FIGURE 1.—Definition of geometrical parameters used in the analysis.

(c) An elastic axis exists in the outer portion of the wing, this axis being defined as the elastic axis the wing would have if it were mounted rigidly some distance outboard of the root approximately perpendicular to the midchord line. (Near the root the elastic axis is defined as the extension of the outboard elastic axis.)

(d) All deformations other than those due to the root rotations are given by the elementary theories of bending and of torsion about the reference axis, which in this case is the elastic axis.

Air loads.—The force on a wing section of unit width parallel to the direction of flight is

$$l=qcc_l \tag{1}$$

or, in matrix notation and in terms of the loading coefficient $\frac{cc_l}{c_r}$,

$$\{l\}=qc_r\left\{\frac{cc_l}{c_r}\right\} \tag{2}$$

The loading coefficient $\frac{cc_l}{c_r}$ at any point on the span can be expressed in terms of the angles of attack at various points on the span by means of aerodynamic influence coefficients. For subsonic speeds, approximate aerodynamic influence coefficients may be calculated by the method of reference 1. With the resulting influence-coefficient matrix $[Q]$, the loading coefficients are given by the relation

$$\left\{\frac{cc_l}{c_r}\right\}=C_{L_\alpha}[Q]\{\alpha\} \tag{3}$$

where α is the total angle of attack, which consists of the sum of the geometrical and structural angles of attack α_g and α_s. The geometrical angle of attack is that due to airplane altitude and built-in twist, whereas the structural angle of attack is that due to structural deformation.

Instead of using the method of reference 1 the matrix $[Q]$ may be calculated more simply (but less accurately) by means of a modified strip theory; the section-lift distribution is rounded at the wing tips and reduced over the entire span by a factor which differs for angles of attack due to attitude and for angles due to any type of twist. On the basis of this approximation

$$\left.\begin{aligned} c_l&=C_{L_\alpha}\alpha_g+C_{L_{\alpha_e}}\alpha_s \\ &=C_{L_\alpha}(\alpha_g+\kappa\alpha_s) \\ &=C_{L_\alpha}\bar{\alpha} \end{aligned}\right\} \tag{4a}$$

for geometrical angles of attack which consist only of the angle of attack due to attitude, and

$$\left.\begin{aligned} c_l&=C_{L_{\alpha_e}}(\alpha_g+\alpha_s) \\ &=C_{L_{\alpha_e}}\alpha \end{aligned}\right\} \tag{4b}$$

for all other geometrical angles of attack (due to rolling, or due to built-in twist, for instance). In equations (4a) and (4b), $C_{L_{\alpha_e}}$ is an effective lift-curve slope for twist distributions and $\bar{\alpha}$ is an effective angle of attack defined by

$$\bar{\alpha}=\alpha_g+\kappa\alpha_s$$

where

$$\kappa=\frac{C_{L_{\alpha_e}}}{C_{L_\alpha}}$$

Approximate values of C_{L_α} and $C_{L_{\alpha_e}}$ may be obtained by the reasoning of references 2 and 3 from the following equations:

$$C_{L_\alpha}=c_{l_\alpha}\frac{A\cos\Lambda}{A+2\cos\Lambda} \tag{5a}$$

$$C_{L_{\alpha_e}}=c_{l_\alpha}\frac{A\cos\Lambda}{A+4\cos\Lambda} \tag{5b}$$

so that

$$\kappa=\frac{A+2\cos\Lambda}{A+4\cos\Lambda} \tag{5c}$$

An influence-coefficient matrix which relates the loading coefficients and angle-of-attack values in the manner indicated in equation (3) may be obtained from equations (4a) and (4b):

$$[Q]=\left[\frac{c}{c_r}\right]\left[(1-\kappa)[1_1]+\kappa[1]\right]$$

where $[1_1]$ is a matrix defined by

$$[1_1]=\begin{bmatrix} 1&0&0&0&.&. \\ 1&0&0&0&.&. \\ 1&0&0&0&.&. \\ 1&0&0&0&.&. \\ .&.&.&.&.&. \\ .&.&.&.&.&. \end{bmatrix}$$

(provided that in the column matrices of α and of $\frac{cc_l}{c_r}$ the values at the wing root or plane of symmetry are written at the top). However, if the modified strip theory is used, equations (4a) and (4b) may be used directly without resorting to an influence-coefficient matrix so that, from equation (4a),

$$\left\{\frac{cc_l}{c_r}\right\}=C_{L_\alpha}\left[\frac{c}{c_r}\right]\{\bar{\alpha}\} \tag{6a}$$

and, from equation (4b),

$$\left\{\frac{cc_l}{c_r}\right\}=C_{L_\alpha}\kappa\left[\frac{c}{c_r}\right]\{\alpha\} \tag{6b}$$

For supersonic speeds the loading coefficient given by unmodified strip theory can be expressed in the form

$$\left\{\frac{cc_l}{c_r}\right\}=c_{l_\alpha}\left[\frac{c}{c_r}\right]\{\alpha\} \tag{6c}$$

where c_{l_α} is the lift-curve slope pertinent to sections perpendicular to the midchord line. For instance, if the two-dimensional lift-curve slope is given by the Ackeret relation

$$c_{l_\alpha}=\frac{4}{\sqrt{M_0^2-1}}$$

then the section lift-curve slope to be used in equation (6c) is

$$c_{l_\alpha}=\frac{4\cos\Lambda_{c/2}}{\sqrt{M_0^2\cos^2\Lambda_{c/2}-1}}$$

In the present report equation (6a) is used for the sake of definiteness. The modifications required in the method to use equations (6b) and (6c) rather than equation (6a) are obvious.

If more accurate aerodynamic influence coefficients than those which correspond to the modified strip theory are desired, the coefficients of reference 1 may be used in the manner described therein. Aerodynamic influence coefficients for subsonic speeds can also be obtained from the theoretical methods of references 4, 5, and 6 for calculating spanwise lift distributions. Whether the increase in accuracy obtainable by combining these methods with that of the present report warrants the corresponding increase in effort is somewhat questionable.

Equations (2) and (6a) may be combined to yield the following relation:

$$\{l\}=C_{L_\alpha}qc_r\left[\frac{c}{c_r}\right]\{\bar{\alpha}\} \tag{7}$$

Similarly, the running torque t may be obtained from the relation

$$t=e_1cl$$

so that

$$\{t\}=C_{L_\alpha}qc_r^2e_{1_r}\left[\frac{e_1}{e_{1_r}}\left(\frac{c}{c_r}\right)^2\right]\{\bar{\alpha}\} \tag{8}$$

(For cambered sections the pitching moment at zero lift must be added and the analysis of the following paragraphs modified accordingly.)

The accumulated torque T is obtained from the running torque and the running load by integrations inboard from the tip. The integration of the running torque may be performed by a matrix $[I']$ which is based on Simpson's rule with a modification suggested by V. M. Falkner at the tip. (See appendix.) The effect of Falkner's modification is to round off the calculated load distribution and cause it to go to zero with an infinite slope at the tip, as the aerodynamic lift distributions at subsonic speeds actually do. For supersonic speeds a similar matrix without tip modification $[I]$ may be used. Both matrices are given in table I. The contribution of the running load to the accumulated torque is equal to the product of $-\tan\Lambda$ and the accumulated bending moment.

The accumulated bending moment M is obtained by a double integration of the running load. The double integration inboard from the tip may be performed by means of the matrices $[II]$ and $[II']$ (given in table II), which are based on the equivalent of Simpson's rule for moments, Falkner's modification again being made at the tip in the case of $[II']$. The derivation of the integrating matrices is discussed in the appendix.

In the following paragraphs subsonic flow will be assumed for the sake of definiteness. For supersonic flow, matrices $[I]$ and $[II]$ are used instead of $[I']$ and $[II']$. The accumulated torque and bending moment may then be written as

$$\{T\}=\frac{b'}{2}[I']\{t\}-\tan\Lambda\{M\} \tag{9}$$

and

$$\{M\}=\left(\frac{b'}{2}\right)^2[II']\{l\} \tag{10}$$

The bending moments and torques referred to the elastic or reference axis, M_A and T_A, can be obtained from those given in equations (9) and (10) by means of the relations

$$\begin{aligned}\{M_A\}&=\cos\Lambda\{M\}-\sin\Lambda\{T\}\\&=\frac{1}{\cos\Lambda}\left(\frac{b'}{2}\right)^2[II']\{l\}-\sin\Lambda\left(\frac{b'}{2}\right)[I']\{t\}\\&=C_{L_\alpha}qc_r\left(\frac{b'}{2}\right)^2\frac{1}{\cos\Lambda}\left[[II']\left[\frac{c}{c_r}\right]-\right.\\&\qquad\left.\sin\Lambda\cos\Lambda\frac{e_{1_r}c_r}{b'/2}[I']\left[\frac{e_1}{e_{1_r}}\left(\frac{c}{c_r}\right)^2\right]\right]\{\bar{\alpha}\}\end{aligned} \tag{11}$$

$$\begin{aligned}\{T_A\}&=\cos\Lambda\{T\}+\sin\Lambda\{M\}\\&=\cos\Lambda\frac{b'}{2}[I']\{t\}\\&=C_{L_\alpha}qc_r^2e_{1_r}\frac{b'}{2}\cos\Lambda[I']\left[\frac{e_1}{e_{1_r}}\left(\frac{c}{c_r}\right)^2\right]\{\bar{\alpha}\}\end{aligned} \tag{12}$$

Structural deformations.—The equations of equilibrium of a deformed wing referred to the elastic axis are

$$GJ\frac{d\varphi}{dy}=T_A \tag{13}$$

$$EI\frac{d\Gamma}{dy}=M_\Lambda \tag{14}$$

These equations must be integrated outboard from the root to obtain φ and Γ. The integrations may be performed by a matrix $[I]''$ (see table III and appendix). Unlike the previously mentioned integrations this one is along the reference axis—that is, with s as the independent variable rather than y or η, which are the independent variables for integrations perpendicular to the plane of symmetry. Consequently, the distance $\frac{b'/2}{\cos\Lambda}$ must be used in conjunction with the dimensionless matrix $[I]''$.

To the deformations obtained in this manner the rotations φ_r and Γ_r due to the deformations of the root triangle must be added. The root rotations may be expressed by four dimensionless constants:

$$Q_{\varphi_T}=\frac{\varphi_{r_T}/T_{\Lambda_r}}{w_e/(GJ)_r} \tag{15a}$$

$$Q_{\varphi_M}=\frac{\varphi_{r_M}/M_{\Lambda_r}}{w_e/(GJ)_r} \tag{15b}$$

$$Q_{\Gamma_T}=\frac{\Gamma_{r_T}/T_{\Lambda_r}}{w_e/(EI)_r} \tag{15c}$$

$$Q_{\Gamma_M}=\frac{\Gamma_{r_M}/M_{\Lambda_r}}{w_e/(EI)_r} \tag{15d}$$

which may be combined into two other constants

$$Q_{\alpha_T}=\frac{\alpha_{r_T}/T_{\Lambda_r}}{w_e/(GJ)_r}=\left(Q_{\varphi_T}-\frac{(GJ)_r}{(EI)_r}\tan\Lambda\, Q_{\Gamma_T}\right)\cos\Lambda \tag{15e}$$

$$Q_{\alpha_M}=\frac{\alpha_{r_M}/M_{\Lambda_r}}{w_e/(GJ)_r}=\left(Q_{\varphi_M}-\frac{(GJ)_r}{(EI)_r}\tan\Lambda\, Q_{\Gamma_M}\right)\cos\Lambda \tag{15f}$$

w_e being defined as in figure 1. The deformations may then be written as

$$\{\varphi\}=\frac{b'/2}{\cos\Lambda(GJ)_r}\left[\left[[I]''\left[\frac{(GJ)_r}{GJ}\right]+\frac{w_e\cos\Lambda}{b'/2}Q_{\varphi_T}[1_l']\right]\{T_\Lambda\}+\frac{w_e\cos\Lambda}{b'/2}Q_{\varphi_M}[1_l']\{M_\Lambda\}\right] \tag{16}$$

and

$$\{\Gamma\}=\frac{b'/2}{\cos\Lambda(EI)_r}\left[\left[[I]''\left[\frac{(EI)_r}{EI}\right]+\frac{w_e\cos\Lambda}{b'/2}Q_{\Gamma_M}[1_l']\right]\{M_\Lambda\}+\frac{w_e\cos\Lambda}{b'/2}Q_{\Gamma_T}[1_l']\{T_\Lambda\}\right] \tag{17}$$

where the matrix $[1_l']$ is defined by

$$[1_l']=\begin{bmatrix}0&0&0&0&.&.\\1&0&0&0&.&.\\1&0&0&0&.&.\\1&0&0&0&.&.\\1&0&0&0&.&.\\.&.&.&.&.&.\\.&.&.&.&.&.\end{bmatrix} \tag{18}$$

The angle of attack due to the structural deformations α_s is related to φ and Γ by

$$\alpha_s=(\varphi-\Gamma\tan\Lambda)\cos\Lambda \tag{19}$$

The aeroelastic equation.—If equations (11), (12), (16), and (17) are substituted in the matrix equivalent of equation (19), the following relation is obtained:

$$\{\alpha_s\}=q^*[A]\{\bar{\alpha}\} \tag{20}$$

where the aeroelastic matrix $[A]$ is defined by

$$[A]=\left[[I]''\left[\frac{(GJ)_r}{GJ}\right]+\frac{w_e}{b'/2}(Q_{\alpha_T}-Q_{\alpha_M}\tan\Lambda)[1_l']+\frac{(GJ)_r}{(EI)_r}(\tan^2\Lambda)[I]''\left[\frac{(EI)_r}{EI}\right]\right][I']\left[\frac{e_1}{e_{1_r}}\left(\frac{c}{c_r}\right)^2\right]-\left[k[I]''\left[\frac{(EI)_r}{EI}\right]-\frac{w_e}{b'/2}\frac{b'/2}{e_{1_r}c_r\cos^2\Lambda}Q_{\alpha_M}[1_l']\right][II']\left[\frac{c}{c_r}\right] \tag{21}$$

the dimensionless dynamic pressure q^*, by

$$q^*=\frac{C_{L_\alpha}q(b'/2)^2e_{1_r}c_r^2\cos\Lambda}{(GJ)_r} \tag{22}$$

and the parameter k, by

$$k=\frac{(GJ)_r}{(EI)_r}\frac{b'/2}{e_{1_r}c_r\cos^2\Lambda}\tan\Lambda \tag{23}$$

(The parameters q^* and k are similar to the parameters a and $\frac{d}{a}$ of reference 2.)

Solution of the aeroelastic equation.—If it is desired to calculate the aerodynamic loading corresponding to a given geometrical angle-of-attack distribution and dynamic pressure, equation (20) may be rewritten as follows:

$$[1]-\kappa q^*[A]]\{\bar{\alpha}\}=\{\alpha_g\} \tag{24}$$

In this form it constitutes a set of linear simultaneous equations for values of $\bar{\alpha}$ in terms of values of α_g. From the calculated values of $\bar{\alpha}$ the lift distribution may be determined from equations (1) and (4).

The divergence dynamic pressure may be obtained from equation (24) by setting the determinant of the square matrix on the left side of the equation equal to zero. This procedure is equivalent to setting α_g equal to zero in the term $\bar{\alpha}$ of equation (20), so that

$$\{\alpha_s\}=\kappa q^*[A]\{\alpha_s\} \tag{25}$$

The critical value of κq^* is then determined by matrix iteration and hence the divergence dynamic pressure from equations (5c) and (22).

METHOD EMPLOYING INFLUENCE COEFFICIENTS

The assumptions made in the preceding sections concerning the behavior of the wing structure are unnecessary if influence coefficients for the given structure are available from test data or refined methods of calculation. The coefficients most convenient for this analysis are those giving

the rotation of the structure in planes parallel to the direction of flight due to vertical loads applied along a convenient reference axis and due to torques about lines perpendicular to the direction of flight.

Since it is usually more convenient to apply concentrated rather than distributed loads in structural tests, the influence coefficients are considered in this analysis to have been obtained in this manner. These coefficients must be converted to coefficients which pertain to distributed loadings. This conversion may be accomplished either by means of the weighting matrices of reference 7 or by means of the conversion matrices described in this section.

The angle of structural deformation α_s may be expressed in terms of the influence coefficients Φ_T and Φ_P as follows:

$$\{\alpha_s\}=[\Phi_T]\{T_c\}+[\Phi_P]\{P\} \tag{26}$$

where the T_c's and P's are arbitrary concentrated torques and loads, the latter being applied at the reference axis. The accumulated torques and bending moments about lines perpendicular and parallel, respectively, to the direction of flight may be related to the concentrated torques and loads by means of the summation matrices $[C_1]$ and $[C_2]$ (see appendix) as follows:

$$\{T\}=[C_1]\{T_c\}-\tan\Lambda\{M\} \tag{27}$$

$$\{M\}=\frac{b'}{2}[C_2]\{P\} \tag{28}$$

These relations may be solved for the values of T_c and P required to produce given distributions of accumulated torque and bending moment

$$\{T_c\}=[C_1]^{-1}\left\{\{T\}+\tan\Lambda\{M\}\right\} \tag{29}$$

$$\{P\}=\frac{1}{b'/2}[C_2]^{-1}\{M\} \tag{30}$$

The accumulated torques and bending moments produced by the air load are then

$$\{T\}=\frac{b'}{2}[I']\{le_1c\}-\{M\}\tan\Lambda \tag{31}$$

$$\{M\}=\left(\frac{b'}{2}\right)^2[II']\{l\} \tag{32}$$

Upon substituting equations (29), (30), (31), (32), (1), and (4) into equation (26), the following equation is obtained:

$$\{\alpha_s\}=q^\dagger[A^\dagger]\{\bar{\alpha}\} \tag{33}$$

where

$$q^\dagger=C_{L_\alpha}q\frac{b'}{2}c_r \tag{34}$$

and

$$[A^\dagger]=\left[e_{1_r}c_r[\Phi_T][C_3']\left[\frac{e_1}{e_{1_r}}\left(\frac{c}{c_r}\right)^2\right]+[\Phi_P][C_4']\left[\frac{c}{c_r}\right]\right] \tag{35}$$

where, in turn

$$[C_3']=[C_1]^{-1}[I'] \tag{36}$$

$$[C_4']=[C_2]^{-1}[II'] \tag{37}$$

are given in tables IV and V. (Conversion matrices for supersonic flow $[C_3]$ and $[C_4]$ can be calculated from $[I]$ and $[II]$, if needed, by replacing $[I']$ and $[II']$ with $[I]$ and $[II]$ in equations (36) and (37).)

The solution of equation (33) is obtained in the manner previously described for equation (20).

APPLICATION OF THE METHOD

DETERMINATION OF THE STRUCTURAL PARAMETERS

At the time an aeroelastic analysis is performed no experimental stiffness data are usually available, so that either the calculated stiffness curves or calculated influence coefficients must be used. In order to use the stiffness curves it is necessary to assume the existence of a reasonably straight elastic axis. The location of this axis may be estimated by considering it to be the line connecting the shear centers of the individual sections. If the elastic axis obtained in this manner is not reasonably straight within one or two percent of the chord, the results of the analysis may not be sufficiently reliable.

The stiffnesses GJ and EI do not have much physical significance inboard of the last point where there is a complete cross section of the torsion box. (See fig. 1.) In order to arrive at estimates of the root stiffnesses $(GJ)_r$ and $(EI)_r$, which serve primarily as reference values in this analysis, the stiffness curves have to be extended. It is convenient to consider the stiffnesses to be constant inboard of the last complete section of the torsion box; this procedure should yield conservative values of the root rotations.

The most difficult problem incurred in analyzing the deflections on the basis of stiffness curves appears to be the estimation of the root rotations. As used in this analysis, they are the torsion and bending deflections imposed by the triangular inner portion of the wing and the carry-through bay on the rest of the wing. As seen in figure 2, which is plotted from the data of reference 8, these values are essentially constant along the span, so that they actually constitute rigid-body rotations. (The bending rotations have been obtained by taking the difference in slope between curves calculated by considering the wing to be cantilevered at the effective root—the root used to calculate torsional deformations in reference 8—and the averages of the leading-edge and trailing-edge deflections actually measured. The twists were obtained by subtracting the twists calculated on the basis of the assumed effective root from the measured twists.)

The rotations should, in any practical case, be calculated by analyzing the triangular root and the carry-through bay

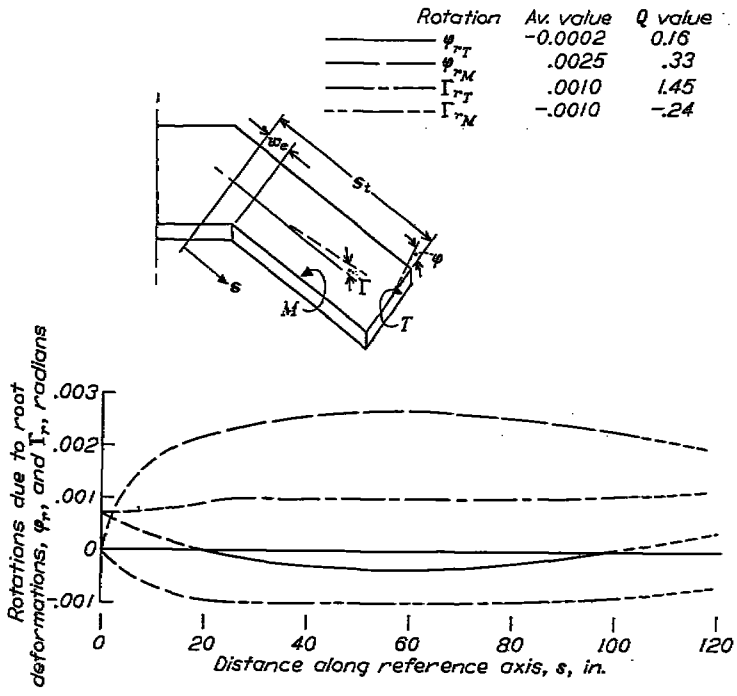

FIGURE 2.—Rotations of a 45° swept box beam due to root deflections (data from reference 8). s_t=104 inches; w_e=15 inches; $(GJ)_r$=5.10×10⁶ pound-inch²; $(EI)_r$=9.47×10⁸ pound-inch²; T_r=43,420 inch-pounds; M_r=260,000 inch-pounds.

and be made dimensionless by means of equations (15a) to (15f). If such an analysis is not available, the dimensionless rotation parameters shown in figure 2 may be used as a guide. It must be kept in mind, however, that in the case of a sweptforward wing the parameters Q_{φ_M} and Q_{Γ_T} would have the opposite sign and that for antisymmetrical loadings the root rotations may be slightly different than for symmetrical loadings (see reference 9).

If higher-order structural effects are to be taken into account—such as shear lag, bending stresses due to torsion, local stresses due to cut-outs, discontinuity of the elastic axis, and so on—structural influence coefficients may be calculated by means of the method of reference 10 and used in the present analysis in the same manner as measured influence coefficients.

Once the structure under investigation is built, fairly simple deflection tests, similar to those performed in references 8 and 9, may be used to check the root-rotation parameters by calculating the differences between the observed rotations and those calculated by simple beam theory considering the wing cantilevered at the effective root; at the same time the existence and estimated location of the elastic axis may be verified. If the experimental program is fairly extensive it is desirable to measure influence coefficients directly. These influence coefficients can then be used in conjunction with the alternate method described in the preceding section to obtain a quick check on the aeroelastic analysis based on calculated stiffnesses.

The influence coefficients used in the analysis consist of the rotations of sections parallel to the direction of flight due to concentrated unit torques in planes parallel to the plane of symmetry or concentrated unit loads at the reference line. When measured, these rotations (in radians) may be entered in tables of the form:

$[\Phi_T]$

TWIST AT STATION $\frac{\eta}{b'/2}$ DUE TO UNIT CONCENTRATED TORQUE AT $\frac{\eta'}{b'/2}$

$\frac{\eta}{b'/2}$ \ $\frac{\eta'}{b'/2}$	0.2	0.4	0.6	0.8	0.9	1.0
0						
0.2						
0.4						
0.6						
0.8						
0.9						

$[\Phi_P]$

TWIST AT STATION $\frac{\eta}{b'/2}$ DUE TO UNIT CONCENTRATED LOAD AT $\frac{\eta'}{b'/2}$

$\frac{\eta}{b'/2}$ \ $\frac{\eta'}{b'/2}$	0.2	0.4	0.6	0.8	0.9	1.0
0						
0.2						
0.4						
0.6						
0.8						
0.9						

These particular tables would be used for a six-point analysis; similar tables would be used for a ten-point analysis. In either case it is to be noted that the twists are measured at values of $\frac{\eta}{b'/2}$ from 0 to 0.9, whereas the loads are applied at values of $\frac{\eta'}{b'/2}$ from 0.2 to 1.0. The tables obtained in this manner constitute the desired influence-coefficient matrices.

If the wing sections are found to twist nonuniformly, so that they become cambered in effect, the angles of twist α_s to be entered in the influence-coefficient matrices have to be

defined in a different manner according to whether the aeroelastic analysis is performed for subsonic or supersonic speeds. At subsonic speeds the lift depends on the slope of the mean camber line at the three-quarter-chord point, so that the effective angle of attack is

$$\alpha_s = 2\frac{(\zeta_{c/2} - \zeta_{TE})}{c} \qquad (38)$$

At supersonic speeds the lift depends primarily on the average slope of the mean camber line, so that

$$\alpha_s = \frac{\zeta_{LE} - \zeta_{TE}}{c} \qquad (39)$$

DETERMINATION OF THE AERODYNAMIC PARAMETERS

The selection of the aerodynamic parameters $C_{L_{\alpha_e}}$ and e_1 for the calculation of the divergence speed has been discussed in reference 2. For calculating the aerodynamic loading at a given flight condition the aerodynamic parameters are chosen for that flight condition. The use of the effective lift-curve slopes C_{L_α} and $C_{L_{\alpha_e}}$ in conjunction with modified strip theory is applicable only to subcritical Mach numbers. At higher speeds no simple span correction is available; neglect of the span correction tends to be conservative for calculation of the divergence speed and the aerodynamic loading, however.

INSTRUCTIONS FOR SOLUTION

Two sets of integrating matrices have been prepared, one for a six-point solution and one for a ten-point solution. The former should be adequate for all practical purposes; only where the stiffness curves are very irregular near the root does the ten-point solution have to be used. The points considered by the two sets of tables in the case of subsonic flow are at $\frac{\eta}{b'/2}$=0, 0.2, 0.4, 0.6, 0.8, and 0.9 for the shorter solution and $\frac{\eta}{b'/2}$=0, 0.1, 0.2, 0.3, 0.4, 0.5, 0.6, 0.7, 0.8, and 0.9 for the longer solution. For supersonic cases an additional point at $\frac{\eta}{b'/2}$=1.0 is used for both solutions. The procedure to be followed for all solutions is identical; although computing forms are presented in this report only for the six-point solution, their extension to the ten-point solution is obvious.

Calculation of the matrices.—The first step in the aeroelastic analysis by means of the stiffness curves is the calculation of the aeroelastic matrix [A] from the physical and geometrical parameters of the wing. These parameters are conveniently tabulated in a form of the type shown in table VI(a). The computation is then carried out according to the instructions of table VI(b), each step in the procedure being identified by the number in the upper left corner of each box. It must be kept in mind that many of the operations call for matrix multiplications where the order of the multiplicands is of importance. (A brief summary of matrix methods is presented in the appendix.) The aeroelastic matrix is obtained as the last step (step 13) of the computations in this form, which constitutes an evaluation of the matrix [A] given in equation (21).

In the computing form of table VI(b) and in the illustrative example the matrices [I'] and [II'] are used for the supersonic case. This procedure results in a slight saving in effort and is justified to a certain extent because even in supersonic flow the reduction of the actual lift carried by a section compared with the strip-theory value is largest at the tip. In general, however, use of the matrices [I] and [II] would probably be preferable for supersonic speeds.

A special case arises when e_{1_r} is zero. If e_1 is not zero along the remainder of the span, its value at some point other than the root may be used as a reference value. The matrix $\left[\frac{e_1}{e_{1_r}}\left(\frac{c}{c_r}\right)^2\right]$ and the multiplying factors of steps 8 and 9 as well as the definition of the parameter q^* are then based on the value of e_1 at this other reference station. If e_1 is zero along the entire span, step 1 and steps 3 to 8 may be omitted and steps 9 to 13 should be modified as follows:

Step 9	$\frac{(EI)_r}{(GJ)_r}\frac{w_s}{b'/2}\frac{Q_{\alpha_M}}{\tan\Lambda}[1_1']$
Step 10	[⑨]—[②]
Step 11	As is
Step 12	Omit
Step 13	$[A]_{e_1=0}$=[⑩][⑪]

If structural influence coefficients of the proper type are available, the calculation of the aeroelastic matrix [$A^\dagger$] is carried out directly by means of equation (35).

Solution for divergence dynamic pressure.—In order to determine the value of the dynamic pressure corresponding to divergence, the aeroelastic matrix [A] or [$A^\dagger$] is iterated (see appendix) as indicated by equation (25). Table VII (a) may be used for this purpose. The result is the critical value of κq^* or $\kappa q^\dagger$. The divergence dynamic pressure is then calculated from equations (22) or (34). (It is to be noted that this pressure will be in pounds per square inch.) Since the aeroelastic matrix is independent of the Mach number, except insofar as e_1 varies with Mach number, the same critical value of κq^* or $\kappa q^\dagger$ may be used to calculate the divergence dynamic pressure for an entire range of Mach numbers. If the value of e_1 changes, however, as it does between the subsonic and supersonic region, critical values of q^* and $q^\dagger$ have to be calculated for both values of e_1.

If the value of e_1 is zero along the entire span and the matrix [A] has been calculated according to the modified instructions, iteration of the matrix will give the value of

the parameter $\kappa\bar{q}$ at divergence. From the definition of $\bar{q}$

$$\kappa\bar{q}=\frac{C_{L_{\alpha_s}} q \left(\frac{b'}{2}\right)^3 c_r \tan \Lambda}{(EI)_r \cos \Lambda} \tag{40}$$

the divergence dynamic pressure may then be calculated.

Solution for aerodynamic loading.—In order to calculate the aerodynamic loading corresponding to a given flight condition and geometric angle-of-attack distribution, the aeroelastic matrix $[A]$ or $[A']$ is multiplied by the value of κq^* or $\kappa q'$ calculated for the given flight condition and subtracted from the unit matrix $[1]$. (See equation (24).) The result may be entered in table VII (b). Again it must be noted that the value of the aeroelastic matrix varies with the flight condition if e_1 varies, so that the aeroelastic matrix corresponding to the proper value of e_1 must be selected.

The elements of the resulting matrix are the coefficients of a set of simultaneous linear algebraic equations for the unknown values of the effective angle-of-attack distribution of the deformed wing $\{\bar{\alpha}\}$ in terms of the known angle-of-attack values of the rigid wing $\{\alpha_s\}$. Table VII (b) is set up for the calculation of the additional loading, the damping-in-roll loading, and a third arbitrary loading; as many loadings as desired may, of course, be calculated by this method. The solution of the equations may be carried out in any convenient manner. The form of table VII (b) has been prepared for use in conjunction with Crout's method of solving linear simultaneous equations (reference 11).

The values of $\bar{\alpha}$ may also be obtained by means of an iterative rather than a simultaneous-equation type of solution. A first approximation to the structural twist may be calculated by premultiplying the column of the values of the geometrical angle of attack α_g by the matrix $[A]$ and multiplying the resulting column by q^*. In so doing, the contribution of α_s to the total equivalent angle $\bar{\alpha}$ has been neglected. However, the approximate values of α_s calculated in this manner may be multiplied by the factor κ and added to the values of the geometrical angle of attack to obtain approximate values of $\bar{\alpha}$. The column of these values is then premultiplied by $q^*[A]$ to obtain a better approximation to α_s. This procedure may be repeated until the solution converges.

Alternatively, the first approximation to the column of α_s may be multiplied by κ and premultiplied by $q^*[A]$ to obtain approximately the contribution of the term α_s in $\bar{\alpha}$ to the calculation of α_s by means of equation (20). In turn, the effect of this contribution on α_s may be calculated by premultiplying the contribution by $\kappa q^*[A]$, and so on. The final value of α_s is then the sum of all these contributions.

Both of these procedures are equivalent. They may be systematized and shortened as follows: The matrix $[A]$ is entered at the upper left of table VII (c). Two sets of values of $\{\alpha_g\}$ are listed at the left of the table. For the rolling case,

$$\alpha_g=\frac{y}{b/2}=\frac{b'}{b}\frac{\eta}{b'/2}+\frac{w}{b} \tag{41}$$

These columns are then premultiplied by the matrix $[A]$. The resulting columns are entered in the columns to the right of the columns of $\{\alpha_g\}$ and again premultiplied by the matrix $[A]$. The results of this second matrix multiplication are entered in the next column and premultiplied again by the matrix $[A]$. This procedure is repeated until all the elements of one column, say the rth, differ from the elements of the preceding column, the $(r-1)$th, only by a constant factor (within 1 percent or less). This constant factor is equal to $\frac{1}{(\kappa q^*)_D}$ and is entered at the bottom of the table. The dimensionless dynamic pressure at divergence is, consequently, obtained automatically in this iterative procedure and need not be calculated separately by means of table VII (a).

The dynamic pressures of interest and the corresponding values of κq^* are entered in the matrix at the upper right of table VII(c). Also entered are the corresponding values of $(\kappa q^*)^2$, $(\kappa q^*)^3$, and so on, up to and including $(\kappa q^*)^{r-1}$. In the next row, however, the values of $\frac{(\kappa q^*)^r}{1-(q/q_D)}$ are entered instead of $(\kappa q^*)^r$.

The values of $\bar{\alpha}$ for the two sets of values of α_g and for the various values of q of interest are then obtained by premultiplying the matrix which consists of the rows κq^*, $(\kappa q^*)^2$, $(\kappa q^*)^3$, . . . (including the row of 1's) by the matrices of the columns $\{\alpha_g\}$, $[A]\{\alpha_g\}$, $[A]^2\{\alpha_g\}$, and so on. The resulting columns comprise the desired values of $\bar{\alpha}$ for the various cases. These values are entered in the appropriate columns of table VII (c).

For most conventional plan forms and structures the results of the iterative procedure described in the foregoing paragraphs converge in two to four cycles ($r=2$ to 4); however, for a wing which is uncommonly flexible near the tip, more cycles may be required. In general, the simultaneous-equation type of solution is preferable when several geometrical angle-of-attack conditions are to be analyzed at one or two dynamic pressures. The iterative procedure, on the other hand, is preferable when only one or two angle-of-attack conditions are to be analyzed for several dynamic pressures. When many stations along the wing span are taken into account, the iterative procedure is preferable in almost all cases.

In the case where e_1 is zero along the span, the headings at the top of table VII (b) should be modified to read

$$\frac{q}{q_D}=\frac{}{[1]-\kappa\bar{q}[A]_{e_1=0}} \qquad q=\frac{}{[1]-\kappa\bar{q}[A]_{e_1=0}} \qquad \kappa\bar{q}=\frac{}{[1]-\kappa\bar{q}[A]_{e_1=0}}$$

where $[A]_{e_1=0}$ has been calculated according to the modified instructions and $\kappa\bar{q}$ has been obtained by iterating $[A]_{e_1=0}$. (See also equation (40).)

The values of $\{\bar{\alpha}\}$ calculated for the additional load distribution ($\alpha_g=1$) constitute values of the ratio $c_{l_{fw}}/c_{l_{rw}}$ or

$(cc_l)_{fw}/(cc_l)_{rw}$ in view of the assumptions made concerning the air forces. The section loading of the flexible wing is obtained from the relation

$$cc_l = cC_{L_\alpha}\bar{\alpha} \tag{42a}$$

or in dimensionless form

$$\frac{cc_l}{c_r} = C_{L_\alpha}\frac{c}{c_r}\bar{\alpha} \tag{42b}$$

The wing lift and the bending moment at the wing root may then be obtained by integrating the load distribution. These integrations may be performed conveniently by multiplying the values of cc_l/c_r by the first rows of the matrices $[I']$ and $[II']$, respectively. Thus

$$L_w = 2qC_{L_\alpha}c_r\frac{b'}{2}[I_1']\left[\frac{c}{c_r}\right]\{\bar{\alpha}\} \tag{43}$$

and

$$M_r = qC_{L_\alpha}c_r\left(\frac{b'}{2}\right)^2[II_1']\left[\frac{c}{c_r}\right]\{\bar{\alpha}\} \tag{44}$$

These quantities may be expressed as dimensionless coefficients:

$$C_{L_w} = \frac{L_w}{qS}$$

and

$$C_{BM} = \frac{4M_r}{qSb}$$

The lateral center of pressure of the wing load $\bar{y}$ may be determined from the relation

$$\bar{y} = \frac{w}{2} + \frac{M_r}{L_w/2} \tag{45}$$

The fore-and-aft location of the aerodynamic center of the wing load measured rearward of the leading edge of the mean aerodynamic chord as a fraction of the mean aerodynamic chord may then be estimated from the relation

$$\frac{a_w}{c_{MAC}} = a + \frac{\bar{y} - y_{MAC}}{c_{MAC}}\tan\Lambda_a \tag{46}$$

where Λ_a is the sweep of the section aerodynamic center line.

For any other geometrical angle-of-attack distributions, such as those due to built-in twist or those due to rolling, the same section lift-curve slope should be used for the geometrical as for the structural deformations, so that C_{L_α} is replaced by $C_{L_{\alpha_e}}$, and κ is unity, and $\bar{\alpha}$ in equations (42) to (44) is replaced by α.

For the damping-in-roll distribution with a tip helix angle of 1 radian, α_s is given by equation (41) and the rolling-moment coefficient due to the wing load is given by

$$C_{l_w} = 2\frac{M_r}{qSb} \tag{47}$$

where M_r is obtained from equation (44) with the values of $\bar{\alpha}$ calculated for this case.

The contribution of the wing to other stability derivatives may be obtained, similarly, by integrating the load distributions due to the angle-of-attack distributions caused by the motion of interest, as described in reference 12; in the case of swept wings, particular care must be taken in selecting the proper angle-of-attack distribution and in accounting for the lateral inclination of the lift vector. (See reference 3.)

If the aerodynamic loading or the stability derivatives are to be obtained for a wide variety of flight conditions, it is convenient to systematize the calculations in the following manner: The aeroelastic matrix is computed for both the subsonic and supersonic aerodynamic-center values and iterated for both cases to obtain the subsonic and supersonic values of the divergence parameter $(\kappa q^*)_D$. From these values the divergence dynamic pressure may be computed by means of equation (22) and plotted against Mach number, as suggested in reference 2; on the same plot, values of the actual dynamic pressure may be plotted against Mach number for various altitudes of interest. Such a plot for a wing, the physical characteristics of which are given in figure 3, is shown in figure 4.

Since at a given Mach number the ratio $\kappa q^*/(\kappa q^*)_D$ is equal to the ratio q/q_D, the range of values of $\kappa q^*/(\kappa q^*)_D$ of interest may be established from this plot for both the subsonic and the supersonic regions. Several representative values of this ratio may then be chosen within the given ranges and the corresponding values of κq^* computed from the previously calculated values of $(\kappa q^*)_D$. The aerodynamic loading is calculated for these values of κq^* by using the appropriate matrix $[A]$ and may be plotted in the form of $(cc_l)_{fw}/(cc_l)_{rw}$, with the ratio q/q_D as a parameter. From these curves (or from the values of $\bar{\alpha}$) the wing lift coefficients may be obtained and plotted in the form $(C_L)_{fw}/(C_L)_{rw}$ against q/q_D; the other coefficients may be obtained and plotted in a similar form.

For any specific flight condition the value of q/q_D may then be obtained from the plot of q and q_D against Mach number. The loading, lift coefficient, or other item of interest may be obtained from the plots which give these items in terms of the rigid-wing values. Once the rigid-wing values at the given Mach number are known, the flexible-wing values may then be obtained immediately.

ILLUSTRATIVE EXAMPLE

In order to illustrate the method described in the preceding sections, a swept wing has been analyzed. The physical and geometrical parameters of the wing are shown in figure 3 and the upper part of table VIII (which follows the form of table VI (a)). The chord, e_1c^2, and stiffness matrices have been obtained from the given parameters and are shown in the lower part of table VIII.

The calculation of the aeroelastic matrix for the subsonic case has been carried out by means of the form of table VI(b). All but three of the steps of the computation are shown in table IX, numbered in the same order as in table VI(b). Steps 1, 2, 6, 7, 11, and 12 constitute matrix multiplications,

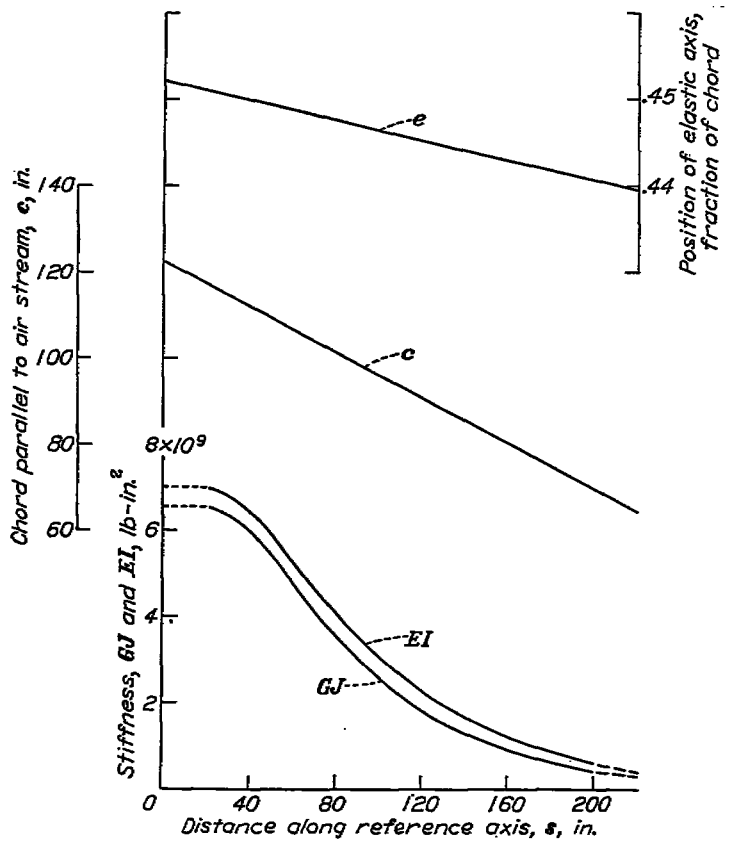

FIGURE 3.—Parameters of the example wing.

which are carried out in the order indicated; steps 5 and 13 constitute matrix additions or subtractions; steps 3 and 4 constitute multiplications of matrices by constants.

The aeroelastic matrix is iterated in table X (a) (which follows the form of table VII (a)) to yield a value of

$$(\kappa q^*)_D = -2.208$$

From this value and a value of this parameter computed in the same manner for supersonic speeds (using $C_{L_\alpha} = C_{L_{\alpha_e}} = c_{l_\alpha}$), the divergence dynamic pressure has been calculated by means of equation (22) on the basis of estimated values of the effective lift-curve slope. The variation with Mach number of the divergence dynamic pressure, the actual dynamic pressure at sea level, and the estimated effective lift-curve slope is shown in figure 4.

For a value of $\frac{q}{q_D} = -0.25$, such as would be obtained approximately at a Mach number of 1.0, the aerodynamic loading has been calculated for the additional-angle-of-attack case and the damping-in-roll case in table X(b), which follows the form of table VII(b). The values of α_e for the damping-in-roll case have been calculated from equation (41). The aerodynamic loadings, in addition to those calculated for other values of q/q_D, have been plotted in figure 5 as ratios of the flexible-wing loadings to the rigid-wing loadings. The curves have been integrated to yield wing lift and rolling-moment coefficients as well as the aerodynamic center of the wing load, which are shown in table X(b) for the case of $\frac{q}{q_D} = -0.25$ and which are plotted against $-\frac{q}{q_D}$ in figure 6.

936646—51——59

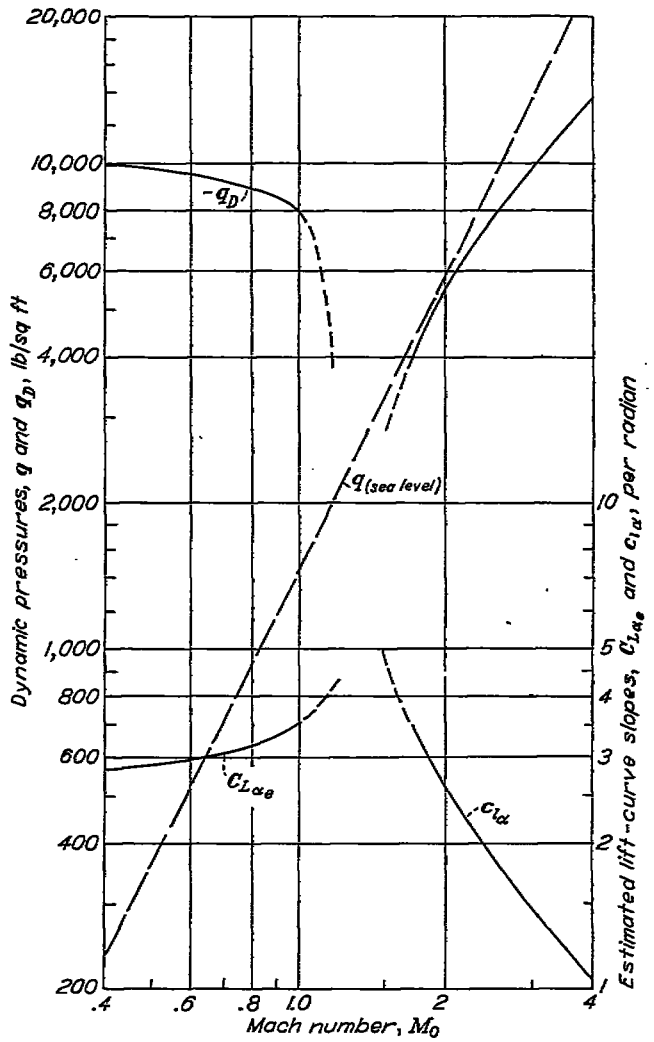

FIGURE 4.—Effect of Mach number on the divergence dynamic pressure and lift-curve slope of the example wing.

The wing lift coefficient is defined in such a manner that if the fuselage lift is known and made dimensionless by dividing by q and S the resulting fuselage lift coefficient may be added directly to the wing lift coefficient. This definition and the fact that figure 5 (a) is plotted over the fraction of the wing-alone span $\frac{b'}{2}$ explain the fact that the area under the curve of figure 5 (a) is not 1. The aerodynamic center as plotted in figure 6 constitutes the center of pressure of only the wing load. In order to obtain the airplane aerodynamic center, the magnitude and center of pressure of the fuselage load would have to be known and taken into account.

DISCUSSION

Both the aerodynamic and the structural assumptions made in this analysis are somewhat more realistic than those made in reference 2. The device employed in this analysis of calculating the air forces for wing sections parallel to the direction of flight and then transferring them to sections perpendicular to the elastic axis obviates the necessity of replacing the actual wing with one the root and tip of which are perpendicular to the elastic axis for the purpose of analysis.

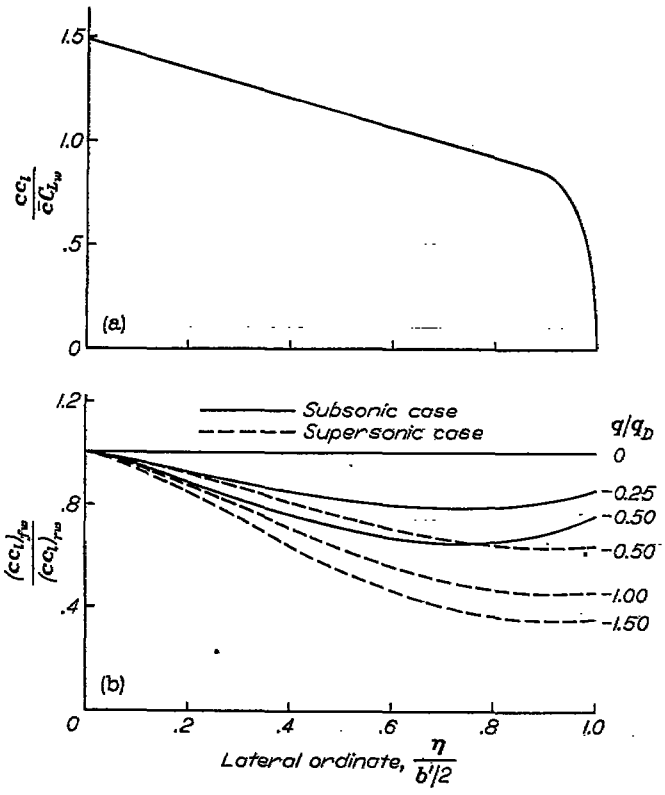

(a) Assumed rigid-wing loading.
(b) Flexible-wing loading.

FIGURE 5.—Load distribution of example wing.

The inclusion of Falkner's modification (see appendix) in the integrating matrices has the effect of rounding off the load distribution approximately in the manner observed at subsonic speeds. At supersonic speeds the load distributions do not go to zero in the same manner, but even at supersonic speeds there is some reduction of load at the tip, the total magnitude of which is not far from the reduction obtained by Falkner's modification. However, the use of special matrices [*I*] and [*II*] is indicated if the amount of this reduction is known.

The assumption, that induction effects may be approximated by an over-all reduction of the strip theory loading (rounded off as previously described) at subcritical speeds and may be neglected at supersonic speeds, may be avoided by using aerodynamic influence-coefficient matrices instead of the effective lift-curve slopes. Available methods of calculating such influence coefficients from theoretical methods for calculating lift distributions for wings of arbitrary plan form at subsonic and supersonic speeds are generally either too inaccurate or too time consuming for practical purposes. The empirical method of reference 1 has the advantage of simplicity and fairly good accuracy compared with theoretical methods but is applicable only to symmetrical lift distributions.

Although the analysis of this report has been performed for wings consisting of uncambered sections, the analysis is directly applicable as well to the determination of the additional loading of wings with cambered sections. The loading of such wings due to the section pitching moment at zero lift may be determined by modifying the analysis somewhat.

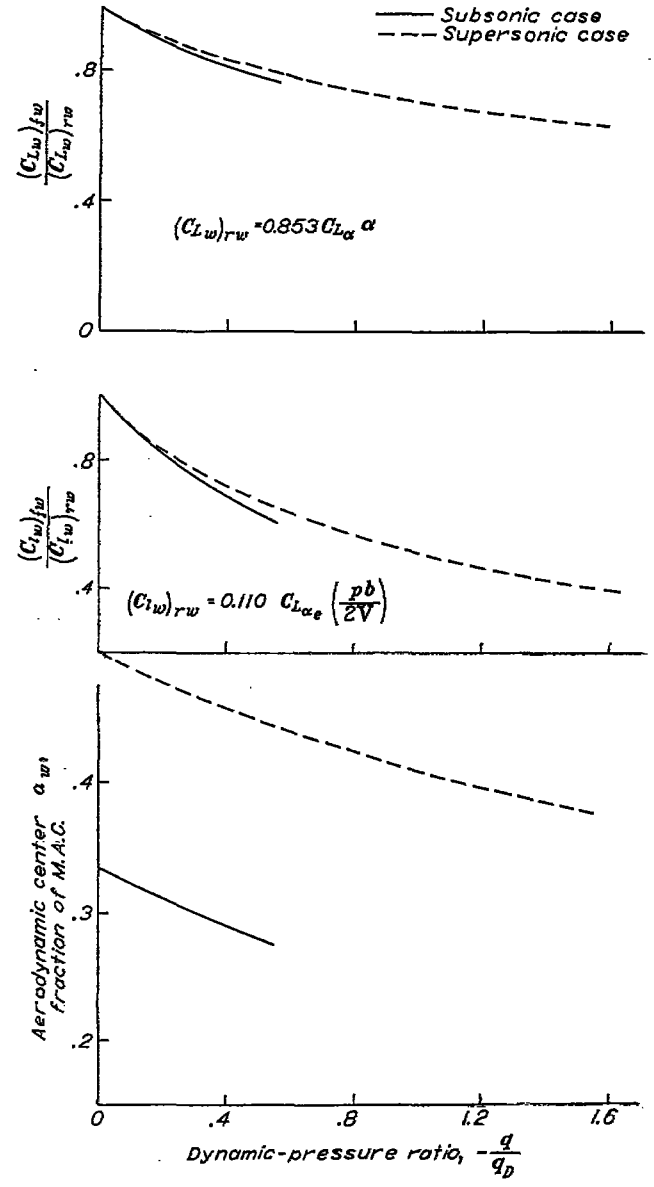

FIGURE 6.—Lift coefficient, rolling-moment coefficient, and aerodynamic center of example wing.

The assumption of an effective root perpendicular to the elastic axis made in reference 2 for the purposes of calculating the structural response is carried over in this analysis. It is modified, however, to the extent that the root is no longer considered to be rigid as in reference 2, but flexible, both in torsion and bending. It has been demonstrated in reference 8 that the deflections of a swept beam may be estimated on that assumption, provided the root-rotation parameters are known. By assuming the effective root at the intersection of the elastic axis with the side of the fuselage, the root bending due to bending moment and root twist due to torque are minimized. The bending due to twist and twist due to bending are the same regardless of the location of the effective root.

The method of introducing the root rotations into the analysis by means of the matrix $[1_r']$ assures that the structural twist in planes parallel to the direction of flight is zero at the fuselage. In so doing the assumption is made that the part of the wing structure within the fuselage does not

deform under load. From figure 2 it is seen that the local values of the root rotation either tend to approach zero at the root or tend to cancel each other. (The root rotations shown in figure 2 do not contain the rotation due to deformation of the carry-through bay; for cases in which this rotation is believed to be sizeable it has to be taken into account in the coefficients Q_{α_M} and Q_{α_T}.) If the root-rotation constants are known, the structural deformations can therefore be predicted quite accurately by the assumptions made.

The manner in which the equations of equilibrium are solved by means of the integrating matrices accounts for the true chord and stiffness variations. It does not necessitate replacement of the actual wing by constant-chord segments with all the flexibility concentrated at the ends of the segments, an approach which has been used extensively in the work on aeroelastic problems of unswept wings.

A further refinement which obviates the necessity for making any structural assumptions other than that of small deflections is the use of measured influence coefficients or coefficients calculated by refined structural theories in the aeroelastic analysis. Wherever such coefficients are available it is, of course, of advantage to use them.

No explicit account has been taken in the analysis of the effects of the inertia loadings on the structural deformations and hence the aerodynamic loading. On swept wings, in particular, their effects may be considerable. For the purposes of this analysis, however, the structural deformations due to inertia loading may be considered part of the geometrical angle of attack and the rigid-wing geometrical angle of attack may be modified accordingly. The deformations due to the inertia loading may, incidentally, be calculated conveniently by means of the matrices $[I]$, $[II]$, and $[I]''$.

Some of the general observations made in reference 2 concerning the divergence phenomenon are corroborated by the example. As expected of a wing with a considerable amount of sweepback, the divergence dynamic pressure is negative; consequently, the wing cannot diverge. The divergence dynamic pressure is useful as a reference value, however; the values of the load distribution and the stability parameters divided either by the corresponding rigid-wing values or by the section lift-curve slope depend only on the ratio of the actual to the divergence dynamic pressure.

The type of plot shown in figure 4 is therefore quite useful in the analysis of aeroelastic phenomena. As pointed out in reference 2, this chart may also be used to estimate the actual divergence dynamic pressure where there is a possibility that the wing may diverge. It appears that the critical values will tend to occur at either extremity of the transonic region.

As would be expected qualitatively, the effect of wing flexibility in the case of the example wing is to unload the wing tips owing to the fact that they bend up. The lift carried by the wing is therefore less than that carried by a rigid wing, the center of pressure being farther inboard and the aerodynamic center being farther forward.

The difference between the supersonic and subsonic values of the loading, the lift and rolling-moment coefficients, and the aerodynamic center for a given value of q/q_D is due to the difference in the values of e_l.

Another item of possible interest is the fact that the variations of the parameters $(\kappa\bar{q})_D$ and $(\kappa q^*)_D$ (the parameters d_D and a_D of reference 2) for the example problem are approximately linear (see fig. 7), as would be expected from the results of the analysis of reference 2. The deviations from linearity are most pronounced near the points for $(\kappa\bar{q})_D=0$ (that is, $\Lambda=0$). They are due to the effects of the root rotations, in particular, the bending due to torsion, and torsion due to bending; these effects were neglected in the approximate analysis of reference 2. The points of figure 7 correspond to the example wing and the wings that would be obtained by rotating the example wing to the unswept and 37.5° sweptforward positions in such a manner as to keep constant the parameters $\frac{e_{l_r}c_r\cos^2\Lambda}{b'/2}$, $\frac{(EI)_r}{(GJ)_r}$, as well as the chord, stiffness, and moment-arm distributions e_l. Points are shown for both the subsonic and supersonic variations as well as for the case when $e_l=0$ over the entire span $((\kappa q^*)_D=0)$. The difference between the subsonic and supersonic lines is due entirely to the difference in the distributions of e_l rather than the difference in the magnitudes of e_{l_r} or in the character of the lift distributions.

The present analysis is concerned only with wing or tail loads; the total loads are obtained by adding the fuselage loads (which may be assumed to be unaffected by flexibility) to the wing or tail loads obtained from the analysis. The amount of load carried by a flexible wing and the manner of its distribution can consequently be estimated by the method presented herein if the contribution of the fuselage is known at low dynamic pressures, that is, for the "rigid-wing" case.

The fuselage has considerable effect on some of the stability parameters, although in the case of others, such as C_{l_p}, the effect is negligible. Other effects that may have to be accounted for in calculating stability derivatives are the boundary-layer behavior and tip suction. The boundary-layer effect may be accounted for by using a section lift-curve slope corrected for boundary-layer effects to calculate

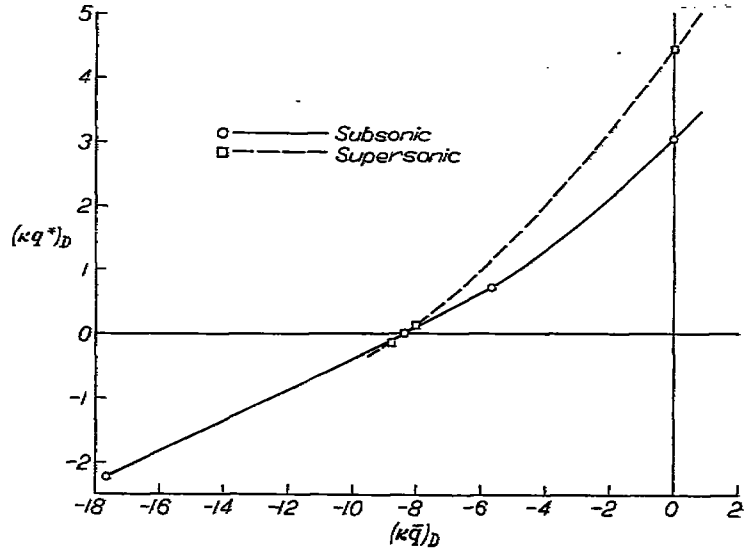

FIGURE 7.—Relation between the parameters $(\kappa q^*)_D$ and $(\kappa\bar{q})_D$.

the angle-of-attack distribution of the flexible wing at the flight conditions of interest and then obtaining the lift and drag distributions corresponding to that angle-of-attack distribution. Lateral tip suction may be important on low-aspect-ratio and highly swept wings. Since this suction does not affect the lift distribution, it may be taken into account by calculating the angle-of-attack distribution of the flexible wing and estimating the tip suction corresponding to the actual angle of attack at the tip.

In calculating stability derivatives it is well to keep in mind that the method presented in this report is based on a modified strip theory, unless aerodynamic influence-coefficient matrices are used. The calculated derivatives may therefore be somewhat in error, particularly if in calculating them the moment of a load distribution has to be determined. If there is reason to suspect that the modified strip theory is inadequate for calculating a given derivative, the derivative may be calculated for the rigid-wing case by a more refined method; the results calculated by the method of this report may then be used to correct the accurate rigid-wing value for the effect of structural flexibility.

CONCLUDING REMARKS

A method has been presented for calculating the aerodynamic loading, the divergence speed, and certain stability derivatives of swept and unswept wings and tail surfaces of arbitrary stiffness. Provisions have been made for using either stiffness curves and root-rotation constants or structural influence coefficients in the structural part of the analysis. Either strip theory with over-all reduction and rounding off at the tip or aerodynamic influence coefficients may be used for the aerodynamic part of the analysis. Computing forms, tables of numerical constants required in the analysis, and an illustrative example are included to facilitate calculations by means of the method.

LANGLEY AERONAUTICAL LABORATORY,
NATIONAL ADVISORY COMMITTEE FOR AERONAUTICS,
LANGLEY FIELD, VA., *December 24, 1948.*

APPENDIX

SUMMARY OF MATRIX ALGEBRA PERTINENT TO THE ANALYSIS

For the convenience of the reader unfamiliar with matrix method, a summary of matrix definitions and operations is presented herein. For a more complete discussion of matrix methods the reader is referred to any text on matrices—for instance, reference 13.

DEFINITIONS

A matrix is a rectangular array of numbers, called elements, written in rows and columns. A column matrix consists of a single column, a row matrix of a single row. A square matrix has as many rows as it has columns.

The diagonal of a square matrix from the upper left to the lower right is called the principal diagonal. A matrix all the elements of which are zero except for those on the principal diagonal is called a diagonal matrix. If all of these elements are unity, the matrix is termed the unit matrix.

The transpose of a square matrix is the square matrix which results from interchanging the rows and columns in the given matrix; it may, consequently, be thought of as having been obtained by rotating the given matrix about its principal diagonal.

MATRIX ALGEBRA

Two matrices can be added or subtracted if both have the same number of rows and columns. The addition or subtraction is carried out by adding to or subtracting from each element of the first matrix the corresponding element of the second matrix.

A matrix is multiplied by a constant by multiplying each element by that constant.

Two matrices can be multiplied by each other if the second has as many rows as the first has columns. Each element of the resulting matrix is obtained by multiplying the elements in the corresponding row of the first matrix by those of the corresponding column of the second matrix in the following order: The first element of the row is multiplied by the first element of the column, the second, by the second, and so forth. The sum of the products obtained in this manner is the value of the element of the product matrix. Schematically this process may be illustrated as follows:

$$\underset{[m]}{\begin{bmatrix} \cdot & \cdot & \cdot & \cdot & \cdot & \cdot & \cdot \\ \cdot & \cdot & \cdot & \cdot & \cdot & \cdot & \cdot \\ a & b & c & d & e & f & g \\ \cdot & \cdot & \cdot & \cdot & \cdot & \cdot & \cdot \\ \cdot & \cdot & \cdot & \cdot & \cdot & \cdot & \cdot \\ \cdot & \cdot & \cdot & \cdot & \cdot & \cdot & \cdot \\ \cdot & \cdot & \cdot & \cdot & \cdot & \cdot & \cdot \end{bmatrix}} \times \underset{[M]}{\begin{bmatrix} \cdot & \cdot & \cdot & \cdot & A & \cdot & \cdot \\ \cdot & \cdot & \cdot & \cdot & B & \cdot & \cdot \\ \cdot & \cdot & \cdot & \cdot & C & \cdot & \cdot \\ \cdot & \cdot & \cdot & \cdot & D & \cdot & \cdot \\ \cdot & \cdot & \cdot & \cdot & E & \cdot & \cdot \\ \cdot & \cdot & \cdot & \cdot & F & \cdot & \cdot \\ \cdot & \cdot & \cdot & \cdot & G & \cdot & \cdot \end{bmatrix}} = \underset{[m][M]}{\begin{bmatrix} \cdot & \cdot & \cdot & \cdot & \cdot & \cdot & \cdot \\ \cdot & \cdot & \cdot & \cdot & \cdot & \cdot & \cdot \\ \cdot & \cdot & \cdot & \cdot & Q & \cdot & \cdot \\ \cdot & \cdot & \cdot & \cdot & \cdot & \cdot & \cdot \\ \cdot & \cdot & \cdot & \cdot & \cdot & \cdot & \cdot \\ \cdot & \cdot & \cdot & \cdot & \cdot & \cdot & \cdot \\ \cdot & \cdot & \cdot & \cdot & \cdot & \cdot & \cdot \end{bmatrix}}$$

where

$$Q=aA+bB+cC+dD+eE+fF+gG$$

It must be emphasized that in multiplying matrices by each other their order is of importance. As the two matrices under consideration are written, the matrix $[m]$ is said to be postmultiplied by the matrix $[M]$, or the matrix $[M]$ may be said to be premultiplied by the matrix $[m]$. If the two matrices were written in the reverse order and then multiplied according to the foregoing instructions—that is, if the

matrix $[M]$ were postmultiplied by the matrix $[m]$—the element of the third row and fifth column of the product matrix $[M][m]$ would clearly not have the value Q in general; nor would, in general, any other element have the value it would have if the two matrices were multiplied in the order shown. Consequently it is important to observe the order in which the matrices are written in the computing instructions.

MATRIX ITERATION

The purpose of iterating a square matrix is to determine the column matrix or matrices which, if postmultiplied by the given square matrix, yield the same column matrix except for a constant multiplier. It is the value or values of these multipliers which constitute the desired characteristic values of the matrix.

The iteration is carried out by assuming a "trial" column (the column shown in table VII (a) is convenient for the purpose of this analysis) and premultiplying it by the given square matrix to yield a "result" column. The elements of the result column including the last are divided by the last element of the result column and entered as a second trial column. The second trial column is then premultiplied by the square matrix to yield a second result column. The procedure is repeated until the same value (within the desired accuracy) is obtained twice in succession for the last element of the result matrix. The reciprocal of this value is the desired (lowest) characteristic value of the matrix, that is, the lowest critical value of $(\kappa q^*)_D$, in the analysis of this report.

Another way of estimating a first trial column in this analysis is to add the elements in each row of the matrix $[A]$, enter the six sums in the first result column, and treat them as if they had been obtained by multiplying the matrix $[A]$ by a first trial column.

DERIVATION OF THE INTEGRATING MATRICES

Although familiarity with the derivation of the integrating matrices is not essential to the application of the method of this report, an outline of the derivation is presented because of its general interest.

The integrating matrices used in this report are based on the same concept as Simpson's rule—replacement of the actual function which is to be integrated by parabolic segments. If the function y has the values y_{n-1}, y_n, and y_{n+1}, respectively, at the equally spaced points x_{n-1}, x_n, and x_{n+1}, the following relations are true for a second-degree parabola passed through the three known points:

$$y=y_n+\frac{1}{2}(y_{n+1}-y_{n-1})\left(\frac{x-x_n}{\Delta x}\right)+\frac{1}{2}(y_{n+1}-2y_n+y_{n-1})\left(\frac{x-x_n}{\Delta x}\right)^2 \tag{A1}$$

$$\int_{x_n-1}^{x_n+1} y\,dx=\left(\frac{1}{3}\Delta x\right)y_{n-1}+\left(\frac{4}{3}\Delta x\right)y_n+\left(\frac{1}{3}\Delta x\right)y_{n+1} \tag{A2}$$

$$\int_{x_n}^{x_n+1} y\,dx=\left(-\frac{1}{12}\Delta x\right)y_{n-1}+\left(\frac{2}{3}\Delta x\right)y_n+\left(\frac{5}{12}\Delta x\right)y_{n+1} \tag{A3}$$

$$\int_{x_n-1}^{x_n} y\,dx=\left(\frac{5}{12}\Delta x\right)y_{n-1}+\left(\frac{2}{3}\Delta x\right)y_n+\left(-\frac{1}{12}\Delta x\right)y_{n+1} \tag{A4}$$

$$\int_{x_n-1}^{x_n+1}(x-x_n)\,y\,dx=\left(-\frac{1}{3}\overline{\Delta x^2}\right)y_{n-1}+(0)\,y_n+\left(\frac{1}{3}\overline{\Delta x^2}\right)y_{n+1} \tag{A5}$$

$$\int_{x_n}^{x_n+1}(x-x_n)\,y\,dx=\left(-\frac{1}{24}\overline{\Delta x^2}\right)y_{n-1}+\left(\frac{1}{4}\overline{\Delta x^2}\right)y_n+\left(\frac{7}{24}\overline{\Delta x^2}\right)y_{n+1} \tag{A6}$$

where

$$\Delta x=x_n-x_{n-1}=x_{n+1}-x_n \tag{A7}$$

The different integrations over the parabolic segments may thus be performed by multiplying the given values of y by the multiplying factors indicated in equations (A2) to (A6).

Since load distributions at subsonic speeds go to zero with infinite slope at the tip and the ordinary second-degree parabola furnishes a poor approximation to such a distribution, V. M. Falkner has suggested that a curve of the type

$$y=A_0+A_1(1-x)^{1/2}+A_2(1-x)^{3/2} \tag{A8}$$

be passed through the last three points of the load-distribution curve at the tip ($x=1$). On the basis of this approximation, relations equivalent to equations (A1) to (A6) may be derived. The multiplying factors for the last two segments are then based on these equivalent expressions rather than those of equations (A2) to (A6).

The integrating factors of equations (A2) to (A6) may be assembled directly into integrating matrices. The matrix $[I]''$, for instance, is set up to perform the integration $\int_0^x y\,dx$. If at the upper limit $x=0.1$ and if the ten-point matrix (table III (b)) is to be used, the factors 0.04167, 0.06667, and −0.00833 may be obtained from equation (A4) since $x_{n-1}=0$, $x_n=0.1$, and $\Delta x=0.1$; similarly, if for the same case the integration is extended to $x_{n+1}=0.2$ as the upper limit, the integrating factors 0.03333, 0.13333, and 0.03333 will be obtained from equation (A2). These factors constitute the second and third rows of the matrix $[I]''$; since the integrations are independent of the values of y other than the first three, the other values of y are multiplied by zero in these two rows. In order to extend the integration to $x=0.3$ an integration is again performed up to $x=0.2$ and another integration, using another parabolic segment, is performed

from $x=0.2$ to $x=0.3$. For the latter integration $x_{n-1}=0.2$, $x_n=0.3$, and $\Delta x=0.1$, so that equation (A4) again yields the factors 0.04167, 0.06667, and −0.00833. The value of y at $x=0.2$ is therefore assigned a multiplying factor of 0.03333 by the first integration and a factor of 0.04167 by the second, or a total factor of 0.07500. The resulting factors are entered in the fourth row of the matrix $[I]''$. All other rows are obtained in a similar manner.

The matrices $[I]$ and $[I']$ are set up to perform the integration $\int_x^1 y\,dx$. The values of the last row of the ten-point matrix $[I']$ (table I (b)) are obtained from the equivalent of equation (A3) for the function given by equation (A8), with $x_{n-1}=0.8$, $x_n=0.9$, $x_{n+1}=1.0$, and $\Delta x=0.1$. Only the multiplying factors for the values of y at $x=0.8$ and $x=0.9$ are listed, since the value of y at $x=1.0$ (the wing tip) is assumed to be zero in this analysis, so that its multiplying factor is immaterial. The values of the last row but one are obtained similarly from the equivalent of equation (A2). The values of the row for $\frac{\eta}{b'/2}=0.7$ are obtained by using equation (A3) in the interval $x=0.6$ to $x=0.8$ and the equivalent of equation (A2) in the interval $x=0.8$ to 1.0. Similarly the row for $\frac{\eta}{b'/2}=0.6$ is obtained by combining the results of equation (A2) for the interval $x=0.6$ to 0.8 with the equivalent of equation (A2) for the interval $x=0.8$ to 1.0. All other rows are obtained in a similar manner.

The matrix $[I]$ is obtained in the same manner as the matrix $[I']$, except that equations (A2) and (A3) are used at the tip instead of their equivalents. This procedure gives rise to a matrix which has one more row and column than the matrix $[I']$. (See tables I and II.) The matrix $[I]$ performs the same operation as the matrix $[I]''$ except for the direction of integration. As a result of this difference the matrix $[I]''$ is essentially a double transpose (first about the principal diagonal, then about the other diagonal) of the matrix $[I]$, as implied by its symbol.

The matrices $[II]$ and $[II']$ are set up to perform the integration $\int_{x_0}^1 (x-x_0)y\,dx$, where x is the variable of integration and x_0, the value of x at the lower limit. In applying the integrating factors of equations (A2) to (A6) to this integration it must be realized that

$$\int (x-x_0)y\,dx=(x_n-x_0)\int y\,dx+\int (x-x_n)y\,dx \qquad (A9)$$

so that the integrating factors for this integration would be obtained by adding (x_n-x_0) times the factors of equation (A2) or (A3) to the factors of equation (A5) or (A6), respectively, the choice of equations depending on the limits of the integration. The factors for the different segments ($x=0.8$ to 1.0, 0.6 to 0.8, and so forth) are then combined for any given row (with its given value of x_0) in the manner indicated for the matrix $[I']$ to yield the matrix $[II']$.

The matrix $[C_1]$ sums up the torques outboard of a given point, whereas the matrix $[C_2]$ gives the sum of the moments of forces applied outboard of a given point. Neither requires any integrations in the sense of equations (A2) to (A6). For the six-point method these two matrices are:

$[C_1]$

$\frac{\eta}{b'/2}$	0.2	0.4	0.6	0.8	0.9	1.0
0	1	1	1	1	1	1
0.2	0	1	1	1	1	1
0.4	0	0	1	1	1	1
0.6	0	0	0	1	1	1
0.8	0	0	0	0	1	1
0.9	0	0	0	0	0	1

$[C_2]$

$\frac{\eta}{b'/2}$	0.2	0.4	0.6	0.8	0.9	1.0
0	0.2	0.4	0.6	0.8	0.9	1.0
0.2	0	.2	.4	.6	.7	.8
0.4	0	0	.2	.4	.5	.6
0.6	0	0	0	.2	.3	.4
0.8	0	0	0	0	.1	.2
0.9	0	0	0	0	0	.1

The moment arms which comprise the matrix $[C_2]$ are fractions of $b'/2$, so that the matrix must be multiplied by the length $b'/2$ in order to yield actual moments, as stated in equation (28).

REFERENCES

1. Diederich, Franklin W.: Approximate Aerodynamic Influence Coefficients for Wings of Arbitrary Plan Form in Subsonic Flow. NACA TN 2092, 1950.
2. Diederich, Franklin W., and Budiansky, Bernard: Divergence of Swept Wings. NACA TN 1680, 1948.
3. Toll, Thomas A., and Queijo, M. J.: Approximate Relations and Charts for Low-Speed Stability Derivatives of Swept Wings. NACA TN 1581, 1948.
4. Multhopp, H.: Die Berechnung der Auftriebsverteilung von Tragflügeln. Luftfahrtforschung, Bd. 15, Lfg. 4, April 6, 1938, pp. 153–169. (Available as R.T.P. Translation No. 2392, British M.A.P.)
5. Weissinger, J.: The Lift Distribution of Swept-Back Wings. NACA TM 1120, 1947.
6. Falkner, V. M.: The Calculation of Aerodynamic Loading on Surfaces of Any Shape. R. & M. No. 1910, British A.R.C., 1943.
7. Benscoter, Stanley V., and Gossard, Myron L.: Matrix Methods for Calculating Cantilever-Beam Deflections. NACA TN 1827, 1949.
8. Zender, George, and Libove, Charles: Stress and Distortion Measurements in a 45° Swept Box Beam Subjected to Bending and to Torsion. NACA TN 1525, 1948.
9. Zender, George W., and Heldenfels, Richard R.: Stress and Distortion Measurements in a 45° Swept Box Beam Subjected to Antisymmetrical Bending and Torsion. NACA TN 2054, 1950.
10. Kuhn, Paul: Deformation Analysis of Wing Structures. NACA TN 1361, 1947.
11. Crout, Prescott D.: A Short Method for Evaluating Determinants and Solving Systems of Linear Equations with Real or Complex Coefficients. Trans. AIEE, vol. 60, 1941, pp. 1235–1240.
12. Pearson, Henry A., and Jones, Robert T.: Theoretical Stability and Control Characteristics of Wings with Various Amounts of Taper and Twist. NACA Rep. 635, 1938.
13. Frazer, R. A., Duncan, W. J., and Collar, A. R.: Elementary Matrices and Some Applications to Dynamics and Differential Equations. The Macmillan Co., 1946.

TABLE I.—VALUES OF THE INTEGRATING MATRICES [I] AND [I']

(a) Six-Point Solution

[I]

$\frac{\eta}{b'/2}$	0	.2	.4	.6	.8	.9	1.0
0	0.06667	0.26667	0.13333	0.26667	0.10000	0.13333	0.03333
.2	−.01667	.13333	.15000	.26667	.10000	.13333	.03333
.4	0	0	.06667	.26667	.10000	.13333	.03333
.6	0	0	−.01667	.13333	.11667	.13333	.03333
.8	0	0	0	0	.03333	.13333	.03333
.9	0	0	0	0	−.00833	.06667	.04167
1.0	0	0	0	0	0	0	0

[I']

$\frac{\eta}{b'/2}$	0	.2	.4	.6	.8	.9
0	0.06667	0.26667	0.13333	0.26667	0.09333	0.15085
.2	−.01667	.13333	.15000	.26667	.09333	.15085
.4	0	0	.06667	.26667	.09333	.15085
.6	0	0	−.01667	.13333	.11000	.15085
.8	0	0	0	0	.02667	.15085
.9	0	0	0	0	−.01886	.09333

(b) Ten-Point Solution

[I']

$\frac{\eta}{b'/2}$	0	.1	.2	.3	.4	.5	.6	.7	.8	.9
0	0.03333	0.13333	0.06667	0.13333	0.06667	0.13333	0.06667	0.13333	0.06000	0.15085
.1	−.00833	.06667	.07500	.13333	.06667	.13333	.06667	.13333	.06000	.15085
.2	0	0	.03333	.13333	.06667	.13333	.06667	.13333	.06000	.15085
.3	0	0	−.00833	.06667	.07500	.13333	.06667	.13333	.06000	.15085
.4	0	0	0	0	.03333	.13333	.06667	.13333	.06000	.15085
.5	0	0	0	0	−.00833	.06667	.07500	.13333	.06000	.15085
.6	0	0	0	0	0	0	.03333	.13333	.06000	.15085
.7	0	0	0	0	0	0	−.00833	.06667	.06833	.15085
.8	0	0	0	0	0	0	0	0	.02667	.15085
.9	0	0	0	0	0	0	0	0	−.01886	.09333

TABLE II.—VALUES OF THE INTEGRATING MATRICES [*II*] AND [*II'*]

(a) Six-Point Solution

[*II*]

$\frac{\eta}{b'/2}$	0	.2	.4	.6	.8	.9	1.0
0	0	0.05333	0.05333	0.16000	0.08000	0.12000	0.03333
.2	−.00167	.01000	.02500	.10667	.06000	.09333	.02667
.4	0	0	0	.05333	.04000	.06667	.02000
.6	0	0	−.00167	.01000	.01833	.04000	.01333
.8	0	0	0	0	0	.01333	.00667
.9	0	0	0	0	−.00042	.00250	.00292
1.0	0	0	0	0	0	0	0

[*II'*]

$\frac{\eta}{b'/2}$	0	.2	.4	.6	.8	.9
0	0	0.05333	0.05333	0.16000	0.07314	0.13792
.2	−.00167	.01000	.02500	.10667	.05448	.10775
.4	0	0	0	.05333	.03581	.07758
.6	0	0	−.00167	.01000	.01548	.04741
.8	0	0	0	0	−.00152	.01724
.9	0	0	0	0	−.00108	.00419

(b) Ten-Point Solution

[*II'*]

$\frac{\eta}{b'/2}$	0	.1	.2	.3	.4	.5	.6	.7	.8	.9
0	0	0.013333	0.013333	0.040000	0.026667	0.066667	0.040000	0.093333	0.046476	0.137620
.1	−.000417	.002500	.006251	.026667	.020000	.053333	.033333	.080000	.040476	.122635
.2	0	0	0	.013333	.013333	.040000	.026667	.066667	.034477	.107750
.3	0	0	−.000417	.002500	.006251	.026667	.020000	.053333	.028476	.092665
.4	0	0	0	0	0	.013333	.013333	.040000	.022476	.077580
.5	0	0	0	0	−.000417	.002500	.006251	.026667	.016477	.062495
.6	0	0	0	0	0	0	0	.013333	.010476	.047410
.7	0	0	0	0	0	0	−.000417	.002500	.004060	.032325
.8	0	0	0	0	0	0	0	0	−.001523	.017240
.9	0	0	0	0	0	0	0	0	−.001077	.004190

TABLE III.—VALUES OF THE INTEGRATING MATRIX [*I*]''

(a) Six-Point Solution

$\frac{\eta}{b'/2}$	0	.2	.4	.6	.8	.9
0	0	0	0	0	0	0
.2	.08333	.13333	−.01667	0	0	0
.4	.06667	.26667	.06667	0	0	0
.6	.06667	.26667	.15000	.13333	−.01667	0
.8	.06667	.26667	.13333	.26667	.06667	0
.9	.06667	.26667	.13333	.26667	.10833	.06667

(b) Ten-Point Solution

$\frac{\eta}{b'/2}$	0	.1	.2	.3	.4	.5	.6	.7	.8	.9
0	0	0	0	0	0	0	0	0	0	0
.1	.04167	.06667	−.00833	0	0	0	0	0	0	0
.2	.03333	.13333	.03333	0	0	0	0	0	0	0
.3	.03333	.13333	.07500	.06667	−.00833	0	0	0	0	0
.4	.03333	.13333	.06667	.13333	.03333	0	0	0	0	0
.5	.03333	.13333	.06667	.13333	.07500	.06667	−.00833	0	0	0
.6	.03333	.13333	.06667	.13333	.06667	.13333	.03333	0	0	0
.7	.03333	.13333	.06667	.13333	.06667	.13333	.07500	.06667	−.00833	0
.8	.03333	.13333	.06667	.13333	.06667	.13333	.06667	.13333	.03333	0
.9	.03333	.13333	.06667	.13333	.06667	.13333	.06667	.13333	.07500	.06667

TABLE IV.—VALUES OF THE LOAD-CONVERSION MATRIX $[C_3']$

(a) Six-Point Solution

$\frac{\eta}{b'/2}$	0	.2	.4	.6	.8	.9
0.2	0.08333	0.13333	−0.01667	0	0	0
.4	−.01667	.13333	.08333	0	0	0
.6	0	0	.08333	.13333	−.01667	0
.8	0	0	−.01667	.13333	.08333	0
.9	0	0	0	0	.04553	.05752
1.0	0	0	0	0	−.01886	.09333

(b) Ten-Point Solution

$\frac{\eta}{b'/2}$	0	.1	.2	.3	.4	.5	.6	.7	.8	.9
0.1	0.04166	0.06667	−0.00833	0	0	0	0	0	0	0
.2	−.00833	.06667	.04167	0	0	0	0	0	0	0
.3	0	0	.04166	.06667	−.00833	0	0	0	0	0
.4	0	0	−.00833	.06667	.04167	0	0	0	0	0
.5	0	0	0	0	.04166	.06667	−.00833	0	0	0
.6	0	0	0	0	−.00833	.06667	.04167	0	0	0
.7	0	0	0	0	0	0	.04166	.06667	−.00833	0
.8	0	0	0	0	0	0	−.00833	.06667	.04167	0
.9	0	0	0	0	0	0	0	0	.04166	0
1.0	0	0	0	0	0	0	0	0	−.00833	.09333

TABLE V.—VALUES OF THE LOAD-CONVERSION MATRIX $[C_4']$

(a) Six-Point Solution

$\frac{\eta}{b'/2}$	0	.2	.4	.6	.8	.9
0.2	0.01667	0.16667	0.01667	0	0	0
.4	−.00833	.05000	.11667	.05000	−.00833	0
.6	0	0	.01667	.16667	.01667	0
.8	0	0	−.00833	.05000	.08946	.02035
.9	0	0	0	0	.00631	.08860
1.0	0	0	0	0	−.01077	.04190

(b) Ten-Point Solution

$\frac{\eta}{b'/2}$	0	.1	.2	.3	.4	.5	.6	.7	.8	.9
0.1	0.00833	0.08333	0.00831	0	0	0	0	0	0	0
.2	−.00417	.02500	.05834	.02500	−.00417	0	0	0	0	0
.3	0	0	.00833	.08333	.00833	0	0	0	0	0
.4	0	0	−.00417	.02500	.05834	.02500	−.00417	0	0	0
.5	0	0	0	0	.00833	.08333	.00833	0	0	0
.6	0	0	0	0	−.00417	.02500	.05834	.02500	−.00417	0
.7	0	0	0	0	0	0	.00833	.08333	.00835	0
.8	0	0	0	0	0	0	−.00417	.02500	.06029	.02035
.9	0	0	0	0	0	0	0	0	.00631	.08860
1.0	0	0	0	0	0	0	0	0	−.01077	.04190

TABLE VI.—FORM FOR COMPUTATION OF AEROELASTIC MATRIX

(a) Wing Parameters

$A=$	$S=$	$w_e=$	$Q_{\varphi_T}=$
$\Lambda=$	$b=$	$\bar{c}=\frac{S}{b}=$	$Q_{\varphi_M}=$
$\tan\Lambda=$	$w=$	a_{sub}	$Q_{\Gamma_T}=$
$\cos\Lambda=$	$b'=$	a_{spr}	$Q_{\Gamma_M}=$

$\frac{\eta}{b'/2}$	η	c	$\bar{c}$	$e_{1_{sub}}$	$e_{1_{spr}}$	GJ	EI
0							
.2							
.4							
.6							
.8							
.9							

$\left[\frac{c}{\bar{c}_r}\right]$

$\frac{\eta}{b'/2}$	0	.2	.4	.6	.8	.9
0	1.000	0	0	0	0	0
.2	0		0	0	0	0
.4	0	0		0	0	0
.6	0	0	0		0	0
.8	0	0	0	0		0
.9	0	0	0	0	0	

$[I_1]$

$\frac{\eta}{b'/2}$	0	.2	.4	.6	.8	.9
0	0	0	0	0	0	0
.2	1	0	0	0	0	0
.4	1	0	0	0	0	0
.6	1	0	0	0	0	0
.8	1	0	0	0	0	0
.9	1	0	0	0	0	0

$\left[\frac{(GJ)_r}{GJ}\right]$

$\frac{\eta}{b'/2}$	0	.2	.4	.6	.8	.9
0	1.000	0	0	0	0	0
.2	0		0	0	0	0
.4	0	0		0	0	0
.6	0	0	0		0	0
.8	0	0	0	0		0
.9	0	0	0	0	0	

$\left[\frac{(EI)_r}{EI}\right]$

$\frac{\eta}{b'/2}$	0	.2	.4	.6	.8	.9
0	1.000	0	0	0	0	0
.2	0		0	0	0	0
.4	0	0		0	0	0
.6	0	0	0		0	0
.8	0	0	0	0		0
.9	0	0	0	0	0	

$\left[\frac{e_1}{e_{1_r}}\left(\frac{c}{\bar{c}_r}\right)^2\right]_{sub}$

$\frac{\eta}{b'/2}$	0	.2	.4	.6	.8	.9
0	1.000	0	0	0	0	0
.2	0		0	0	0	0
.4	0	0		0	0	0
.6	0	0	0		0	0
.8	0	0	0	0		0
.9	0	0	0	0	0	

$\left[\frac{e_1}{e_{1_r}}\left(\frac{c}{\bar{c}_r}\right)^2\right]_{spr}$

$\frac{\eta}{b'/2}$	0	.2	.4	.6	.8	.9
0	1.000	0	0	0	0	0
.2	0		0	0	0	0
.4	0	0		0	0	0
.6	0	0	0		0	0
.8	0	0	0	0		0
.9	0	0	0	0	0	

TABLE VI.—FORM FOR COMPUTATION OF AERODYNAMIC MATRIX—Continued

(b) Computing Instructions

①	$[I]''\left[\frac{(GJ)_r}{GJ}\right]$					
$\frac{\eta}{b'/2}$	0	.2	.4	.6	.8	.9
0	0	0	0	0	0	0
.2	.08333			0	0	0
.4	.06667			0	0	0
.6	.06667					0
.8	.06667					0
.9	.06667					

②	$[I]''\left[\frac{(EI)_r}{EI}\right]$					
$\frac{\eta}{b'/2}$	0	.2	.4	.6	.8	.9
0	0	0	0	0	0	0
.2	.08333			0	0	0
.4	.06667			0	0	0
.6	.06667					0
.8	.06667					0
.9	.06667					

③	$\frac{(GJ)_r}{(EI)_r}(\tan^2\Lambda)$ [②]					
$\frac{\eta}{b'/2}$	0	.2	.4	.6	.8	.9
0	0	0	0	0	0	0
.2				0	0	0
.4				0	0	0
.6						0
.8						0
.9						

$\frac{(GJ)_r}{(EI)_r}\tan^2\Lambda =$ _____

④	$\frac{w_e}{b'/2}\left(Q_{\alpha_T}-Q_{\alpha_M}\tan\Lambda\right)[l_1']$					
$\frac{\eta}{b'/2}$	0	.2	.4	.6	.8	.9
0	0	0	0	0	0	0
.2		0	0	0	0	0
.4		0	0	0	0	0
.6		0	0	0	0	0
.8		0	0	0	0	0
.9		0	0	0	0	0

$\frac{w_e}{b'/2}\left(Q_{\alpha_T}-Q_{\alpha_M}\tan\Lambda\right) =$ _____

⑤	[③]+[③]+[②]					
$\frac{\eta}{b'/2}$	0	.2	.4	.6	.8	.9
0	0	0	0	0	0	0
.2				0	0	0
.4				0	0	0
.6						0
.8						0
.9						

⑥	$[I']\left[\frac{e_1}{e_{1_r}}\left(\frac{c}{c_r}\right)^2\right]_{sub}$					
$\frac{\eta}{b'/2}$	0	.2	.4	.6	.8	.9
0	0.06667					
.2	−.01667					
.4	0	0				
.6	0	0				
.8	0	0	0	0		
.9	0	0	0	0		

⑦	[⑥] [⑥]					
$\frac{\eta}{b'/2}$	0	.2	.4	.6	.8	.9
0	0	0	0	0	0	0
.2						
.4						
.6						
.8						
.9						

⑧	k [②]					
$\frac{\eta}{b'/2}$	0	.2	.4	.6	.8	.9
0	0	0	0	0	0	0
.2				0	0	0
.4				0	0	0
.6						0
.8						0
.9						

$k = \frac{(GJ)_r}{(EI)_r}\frac{b'/2}{e_{1_r}c_r\cos^2\Lambda}\tan\Lambda =$ _____

TABLE VI.—FORM FOR COMPUTATION OF AEROELASTIC MATRIX—Continued

(b) Computing Instructions—Continued

⑨	$\frac{w_e}{b'/2}\frac{b'/2}{e_{l_r}c_r\cos^2\Lambda}Q_{\alpha_M}[l_1']$					
$\frac{\eta}{b'/2}$	0	.2	.4	.6	.8	.9
0	0	0	0	0	0	0
.2		0	0	0	0	0
.4		0	0	0	0	0
.6		0	0	0	0	0
.8		0	0	0	0	0
.9		0	0	0	0	0

$\frac{w_e}{b'/2}\frac{b'/2}{e_{l_r}c_r\cos^2\Lambda}Q_{\alpha_M}=$ _____

⑩	[⑧]−[⑨]					
$\frac{\eta}{b'/2}$	0	.2	.4	.6	.8	.9
0	0	0	0	0	0	0
.2				0	0	0
.4				0	0	0
.6						0
.8						0
.9						

Subsonic Case

⑪	$[II']\left[\frac{c}{c_r}\right]$					
$\frac{\eta}{b'/2}$	0	.2	.4	.6	.8	.9
0	0					
.2	−.00167					
.4	0	0	0			
.6	0	0				
.8	0	0	0	0		
.9	0	0	0	0		

⑫	[⑩] [⑪]					
$\frac{\eta}{b'/2}$	0	.2	.4	.6	.8	.9
0	0	0	0	0	0	0
.2						
.4						
.6						
.8						
.9						

⑬	[A]=[⑦]−[⑫]					
$\frac{\eta}{b'/2}$	0	.2	.4	.6	.8	.9
0	0	0	0	0	0	0
.2						
.4						
.6						
.8						
.9						

TABLE VI.—FORM FOR COMPUTATION OF AERODYNAMIC MATRIX—Concluded

(b) Computing Instructions—Concluded

Supersonic Case

⑥a	$[I']\left[\frac{e_1}{e_{1_r}}\left(\frac{c}{c_r}\right)^2\right]_{spr}$					
$\frac{\eta}{b'/2}$	0	.2	.4	.6	.8	.9
0	0.06667					
.2	−.01667					
.4	0	0				
.6	0	0				
.8	0	0	0	0		
.9	0	0	0	0		

⑫a	$\frac{(e_{1_r})_{sub}}{(e_{1_r})_{spr}}$ [⑫]					
$\frac{\eta}{b'/2}$	0	.2	.4	.6	.8	.9
0	0	0	0	0	0	0
.2						
.4						
.6						
.8						
.9						

$\frac{(e_{1_r})_{sub}}{(e_{1_r})_{spr}}$ = _____

⑦a	[⑤] [⑥a]					
$\frac{\eta}{b'/2}$	0	.2	.4	.6	.8	.9
0	0	0	0	0	0	0
.2						
.4						
.6						
.8						
.9						

⑬a	[A]=[⑦a]−[⑫a]					
$\frac{\eta}{b'/2}$	0	.2	.4	.6	.8	.9
0	0	0	0	0	0	0
.2						
.4						
.6						
.8						
.9						

TABLE VII.—FORM FOR SOLUTION OF AEROELASTIC EQUATION

(a) Divergence

$[A]$						
$\frac{\eta}{b'/2}$	0	.2	.4	.6	.8	.9
0	0	0	0	0	0	0
.2						
.4						
.6						
.8						
.9						

$\{\alpha_s\}$						
$\frac{\eta}{b'/2}$	(1)	(2)	(3)	(4)	(5)	(6)
0	0	0	0	0	0	0
.2	.3000					
.4	.5000					
.6	.7000					
.8	.9000					
.9	1.0000	1.0000	1.0000	1.0000	1.0000	1.0000

$[A]\{\alpha_s\}$						
$\frac{\eta}{b'/2}$	(1)	(2)	(3)	(4)	(5)	(6)
0	0	0	0	0	0	0
.2						
.4						
.6						
.8						
.9						

$(kq^*)_D$=____

TABLE VII.—FORM FOR SOLUTION OF AERODYNAMIC EQUATION—Continued

(b) Aerodynamic Loading

$\frac{q}{q_D}$=____ q=____ κq^*=____

$[[1]-\kappa q^*[A]]$						
$\frac{\eta}{b'/2}$	0	.2	.4	.6	.8	.9
0	1.0000	0	0	0	0	0
.2						
.4						
.6						
.8						
.9						

$\{\alpha_g\}$	$\{\alpha_g\}$	$\{\alpha_g\}$
1		
1		
1		
1		
1		
1		

Auxiliary matrices

0	1.0000	0	0	0	0	0
.2						
.4						
.6						
.8						
.9						

	1.0000		

$[F_1]$ $[c/c_r]$							
①							

$[II'_1]$ $[c/c_r]$							
③							

Final matrices

$\{\bar{\alpha}\}$	$\{\bar{\alpha}\}$	$\{\bar{\alpha}\}$

$[⑤]\{\bar{\alpha}\}$=____	$[⑥]\{\bar{\alpha}\}$=____	$[⑥]\{\bar{\alpha}\}$=____
$[③]\{\bar{\alpha}\}$=____	$[③]\{\bar{\alpha}\}$=____	$[③]\{\bar{\alpha}\}$=____

C_{L_w}=____	C_{BM_w}=____	C_{l_w}=____	$\frac{\bar{\eta}}{b'/2}$=____

TABLE VII.—FORM FOR SOLUTION OF AEROELASTIC EQUATION—Concluded

(c) Solution by Iteration

$\frac{\eta}{b'/2}$	$[A]$					
0						
.2						
.4						
.6						
.8						
.9						

q				
$\frac{}{}$	1	1	1	1
κq^*				
$(\kappa q^*)^2$				
$(\kappa q^*)^3$				
$\frac{(\kappa q^*)^r}{1-(q/q_D)}$				

$\frac{\eta}{b'/2}$	$\{\alpha_g\}$	$[A]\{\alpha_g\}$	$[A]^2\{\alpha_g\}$	$[A]^3\{\alpha_g\}$		$[A]^r\{\alpha_g\}$		$\{\bar{\alpha}\}$	$\{\bar{\alpha}\}$	$\{\bar{\alpha}\}$	$\{\bar{\alpha}\}$
0							Geometrical angle of attack due to air-plane altitude				
.2											
.4											
.6											
.8											
.9											
0							Geometrical angle of attack due to roll				
.2											
.4											
.6											
.8											
.9											

$\frac{1}{(\kappa Q^*)_D}$=_____ $(\kappa q^*)_D$=_____

TABLE VIII.—PARAMETERS OF EXAMPLE WING

$A=4$	$S=3749S$	$w_e=22.4$	$Q_{\sigma_T}=0$
$\Lambda=37.5^\circ$	$b=387.4$	$\bar{c}=\frac{S}{b}=96.8$	$Q_{\sigma_M}=0.40$
$\tan\Lambda=0.7673$	$w=43$	$a_{sub}=0.25$	$Q_{\Gamma_T}=1.60$
$\cos\Lambda=0.7934$	$b'=344.4$	$a_{spr}=0.425$	$Q_{\Gamma_M}=-0.25$

$\frac{\eta}{b'/2}$	η	c	e	$e_{1_{sub}}$	$e_{1_{spr}}$	GJ	EI
0	0	122.5	0.4522	0.202	0.0272	6.56×10^9	7.02×10^9
.2	43.8	110.8	.4493	.199	.0243	5.79	6.28
.4	87.6	99.3	.4469	.197	.0219	3.13	3.65
.6	131.3	87.7	.4444	.194	.0194	1.49	1.89
.8	175.1	76.2	.4420	.192	.0170	.68	.94
.9	197.0	70.3	.4407	.191	.0157	.42	.64

$\left\lfloor\frac{c}{c_r}\right\rceil$

$\frac{\eta}{b'/2}$	0	.2	.4	.6	.8	.9
0	1.000	0	0	0	0	0
.2	0	.905	0	0	0	0
.4	0	0	.811	0	0	0
.6	0	0	0	.716	0	0
.8	0	0	0	0	.622	0
.9	0	0	0	0	0	.574

$[1_1']$

$\frac{\eta}{b'/2}$	0	.2	.4	.6	.8	.9
0	0	0	0	0	0	0
.2	1	0	0	0	0	0
.4	1	0	0	0	0	0
.6	1	0	0	0	0	0
.8	1	0	0	0	0	0
.9	1	0	0	0	0	0

$\left\lfloor\frac{(GJ)_r}{GJ}\right\rceil$

$\frac{\eta}{b'/2}$	0	.2	.4	.6	.8	.9
0	1.000	0	0	0	0	0
.2	0	1.13	0	0	0	0
.4	0	0	2.10	0	0	0
.6	0	0	0	4.40	0	0
.8	0	0	0	0	9.64	0
.9	0	0	0	0	0	15.61

$\left\lfloor\frac{(EI)_r}{EI}\right\rceil$

$\frac{\eta}{b'/2}$	0	.2	.4	.6	.8	.9
0	1.00	0	0	0	0	0
.2	0	1.12	0	0	0	0
.4	0	0	1.92	0	0	0
.6	0	0	0	3.71	0	0
.8	0	0	0	0	7.47	0
.9	0	0	0	0	0	10.96

$\left\lfloor\frac{e_1}{e_{1_r}}\left(\frac{c}{c_r}\right)^2\right\rceil_{sub}$

$\frac{\eta}{b'/2}$	0	.2	.4	.6	.8	.9
0	1.000	0	0	0	0	0
.2	0	.806	0	0	0	0
.4	0	0	.642	0	0	0
.6	0	0	0	.492	0	0
.8	0	0	0	0	.368	0
.9	0	0	0	0	0	.312

$\left\lfloor\frac{e_1}{e_{1_r}}\left(\frac{c}{c_r}\right)^2\right\rceil_{spr}$

$\frac{\eta}{b'/2}$	0	.2	.4	.6	.8	.9
0	1.000	0	0	0	0	0
.2	0	.732	0	0	0	0
.4	0	0	.530	0	0	0
.6	0	0	0	.366	0	0
.8	0	0	0	0	.242	0
.9	0	0	0	0	0	.190

TABLE IX.—COMPUTATION OF AEROELASTIC MATRIX OF EXAMPLE WING (SUBSONIC CASE)

①	$[I]''\left[\frac{(GJ)_r}{GJ}\right]$					
$\frac{\eta}{b'/2}$	0	.2	.4	.6	.8	.9
0	0	0	0	0	0	0
.2	.08333	.15066	−.02501	0	0	0
.4	.06667	.30134	.14001	0	0	0
.6	.06667	.30134	.31500	.58665	−.16070	0
.8	.06667	.30134	.27999	1.17335	.64270	0
.9	.06667	.30134	.27999	1.17335	1.04430	1.04072

②	$[I]''\left[\frac{(EI)_r}{EI}\right]$					
$\frac{\eta}{b'/2}$	0	.2	.4	.6	.8	.9
0	0	0	0	0	0	0
.2	.08333	.14933	−.03201	0	0	0
.4	.06667	.29867	.12801	0	0	0
.6	.06667	.29867	.28800	.49465	−.12452	0
.8	.06667	.29867	.25599	.98935	.49802	0
.9	.06667	.29867	.25599	.98935	.80923	.73070

③	$\frac{(GJ)_r}{(EI)_r}(\tan^2\Lambda)\,[②]$					
$\frac{\eta}{b'/2}$	0	.2	.4	.6	.8	.9
0	0	0	0	0	0	0
.2	.04585	.08216	−.01761	0	0	0
.4	.03668	.16433	.07043	0	0	0
.6	.03668	.16433	.15846	.27216	−.06851	0
.8	.03668	.16433	.14085	.54434	.27401	0
.9	.03668	.16433	.14085	.54434	.44524	.40203

$\frac{(GJ)_r}{(EI)_r}\tan^2\Lambda = 0.5502$

④	$\frac{w_e}{b'/2}(Q_{\alpha_T}-Q_{\alpha_M}\tan\Lambda)\,[l_1']$					
$\frac{\eta}{b'/2}$	0	.2	.4	.6	.8	.9
0	0	0	0	0	0	0
.2	−.1629	0	0	0	0	0
.4	−.1629	0	0	0	0	0
.6	−.1629	0	0	0	0	0
.8	−.1629	0	0	0	0	0
.9	−.1629	0	0	0	0	0

$\frac{w_e}{b'/2}(Q_{\alpha_T}-Q_{\alpha_M}\tan\Lambda) = -0.1629$

⑤	[①]+[③]+[④]					
$\frac{\eta}{b'/2}$	0	.2	.4	.6	.8	.9
0	0	0	0	0	0	0
.2	−.03372	.23282	−.05262	0	0	0
.4	−.05955	.46567	.21044	0	0	0
.6	−.05955	.46567	.47346	.85881	−.22921	0
.8	−.05955	.46567	.42084	1.71769	.91671	0
.9	−.05955	.46567	.42084	1.71769	1.48954	1.44275

⑥	$[I']\left[\frac{e_1}{e_{1_r}}\left(\frac{c}{c_r}\right)^3\right]_{sub}$					
$\frac{\eta}{b'/2}$	0	.2	.4	.6	.8	.9
0	0.06667	0.21494	0.08560	0.13120	0.03435	0.04707
.2	−.01667	.10746	.09630	.13120	.03435	.04707
.4	0	0	.04280	.13120	.03435	.04707
.6	0	0	−.01070	.06560	.01018	.04707
.8	0	0	0	0	.00981	.04707
.9	0	0	0	0	−.00694	.02912

⑦	[⑤][⑥]					
$\frac{\eta}{b'/2}$	0	.2	.4	.6	.8	.9
0	0	0	0	0	0	0
.2	−.00613	.01777	.01728	.01922	.00503	.00689
.4	−.01173	.03724	.04875	.08089	.02118	.02902
.6	−.01173	.03724	.05052	.17174	.06273	.07104
.8	−.01173	.03724	.03938	.22118	.10693	.16293
.9	−.01173	.03724	.03938	.22118	.10254	.23190

⑪	$[II']\left[\frac{c}{c_r}\right]$					
$\frac{\eta}{b'/2}$	0	.2	.4	.6	.8	.9
0	0	0.04826	0.04325	0.11456	0.04549	0.07917
.2	−.00167	.00905	.02028	.07638	.03359	.06185
.4	0	0	0	.03818	.02227	.04453
.6	0	0	−.00135	.00716	.00963	.02721
.8	0	0	0	0	−.00095	.00990
.9	0	0	0	0	−.00067	.00241

⑫	[⑩][⑪]					
$\frac{\eta}{b'/2}$	0	.2	.4	.6	.8	.9
0	0	0	0	0	0	0
.2	−.00199	.01106	.02444	.08202	.03500	.06256
.4	−.00399	.01543	.04289	.20681	.09790	.18314
.6	−.00399	.01543	.03755	.28397	.16542	.33756
.8	−.00399	.01543	.03221	.30252	.19308	.48336
.9	−.00399	.01543	.03221	.30252	.18680	.52203

⑬	[A]=[⑦]−[⑫]					
$\frac{\eta}{b'/2}$	0	.2	.4	.6	.8	.9
0	0	0	0	0	0	0
.2	−.00414	.00671	−.00716	−.00280	−.02997	−.05597
.4	−.00774	.02181	.00536	−.12592	−.07672	−.15412
.6	−.00774	.02181	.01327	−.11223	−.10269	−.26682
.8	−.00774	.02181	.00717	−.08134	−.08615	−.32043
.9	−.00774	.02181	.00717	−.08134	−.08426	−.29018

TABLE X.—SOLUTION OF AEROELASTIC EQUATION FOR EXAMPLE WING (SUBSONIC CASE)

(a) Divergence

$[A]$

$\frac{\eta}{b'/2}$	0	.2	.4	.6	.8	.9
0	0	0	0	0	0	0
.2	−.0041	.0067	−.0072	−.0628	−.0800	−.0560
.4	−.0077	.0218	.0059	−.1259	−.0767	−.1541
.6	−.0077	.0218	.0133	−.1122	−.1027	−.2668
.8	−.0077	.0218	.0072	−.0813	−.0862	−.3204
.9	−.0077	.0218	.0072	−.0813	−.0848	−.2902

$\{\alpha_s\}$

$\frac{\eta}{b'/2}$	(1)	(2)	(3)	(4)	(5)	(6)
0	0	0	0	0	0	0
.2	.3000	.3115	.3449	.3480		
.4	.5000	.7811	.7846	.7876		
.6	.7000	1.0286	1.0526	1.0532		
.8	.9000	1.0775	1.0714	1.0713		
.9	1.0000	1.0000	1.0000	1.0000	1.0000	1.0000

$[A]\{\alpha_s\}$

$\frac{\eta}{b'/2}$	(1)	(2)	(3)	(4)	(5)	(6)
0	0	0	0	0	0	0
.2	−.1286	−.1561	−.1576			
.4	−.3018	−.3551	−.3567			
.6	−.4246	−.4764	−.4770			
.8	−.4448	−.4849	−.4852			
.9	−.4128	−.4526	−.4529	−.4529		

$(\kappa q^*)_D = -2.208$

(b) Aerodynamic Loading

$\frac{q}{q_D} = -0.25 \qquad q = \text{——} \qquad \kappa q^* = 0.552$

$[[1]-\kappa q^*[A]]$

$\frac{\eta}{b'/2}$	0	.2	.4	.6	.8	.9	$\{\alpha_s\}$	$\{\alpha_s\}$	$\{\alpha_s\}$
0	1.0000	0	0	0	0	0	1	0.1083	
.2	.0023	.9963	.0040	.0347	.0165	.0309	1	.2826	
.4	.0043	−.0120	.9968	.0695	.0424	.0851	1	.4620	
.6	.0043	−.0120	−.0073	1.0620	.0567	.1473	1	.6413	
.8	.0043	−.0120	−.0040	.0449	1.0476	.1769	1	.8207	
.9	.0043	−.0120	−.0040	.0449	.0465	1.1602	1	.9103	

Auxiliary matrices

0	1.0000	0	0	0	0	0	1.0000	0.1083	
.2	.0023	.9963	.0040	.0348	.0166	.0310	1.0014	.2834	
.4	.0043	−.0120	.9968	.0702	.0427	.0857	1.0110	.4665	
.6	.0043	−.0120	−.0073	1.0629	.0538	.1395	.9551	.6094	
.8	.0043	−.0120	.0039	.0456	1.0455	.1638	.9261	.7630	
.9	.0043	−.0120	.0039	.0456	.0444	1.1473	.8081	.7439	

Final matrices

$[I'_1]\,[c/c_r]$

							$\{\bar{\alpha}\}$	$\{\bar{\alpha}\}$	$\{\bar{\alpha}\}$
①	0.0667	0.2418	0.1081	0.1909	0.0581	0.0866	1.0000	0.1083	
							.9320	.2320	
							.8518	.3423	
							.7996	.4711	
							.7937	.6412	
							.8081	.7849	

$[II'_1]\,[c/c_r]$

②	0	0.0433	0.0433	0.1146	0.0455	0.0792

$[①]\{\bar{\alpha}\} = 0.6524$	$[①]\{\bar{\alpha}\} =$	$[①]\{\bar{\alpha}\} =$
$[②]\{\bar{\alpha}\} = 0.2736$	$[②]\{\bar{\alpha}\} = 0.1681$	$[②]\{\bar{\alpha}\} =$

$C_{L_w} = 0.740 C_{L_\alpha}$	$C_{BM_w} = 0.277 C_{L_\alpha}$	$C_{l_w} = 0.0855 C_{L_{\alpha_s}}$	$\frac{\bar{\eta}}{b'/2} = 0.419$